Journal of African Earth Sciences 110 (2015) 34–51

Contents lists available at ScienceDirect

Journal of African Earth Sciences

journal homepage: www.elsevier.com/locate/jafrearsci

Facies analysis and depositional environments of the Upper Jurassic Jubaila Formation, Central Saudi Arabia

Hesham M. El-Asmar [a,b], Ehab M. Assal [a], Abdelbaset S. El-Sorogy [c,d,*], Mohamed Youssef [c,e]

[a] Geology Department, Faculty of Science, Damietta University, New Damietta City, 34517 Damietta, Egypt
[b] King Saud University, Saudi Arabia
[c] Department of Geology and Geophysics, College of Science, King Saud University, Saudi Arabia
[d] Geology Department, Faculty of Science, Zagazig University, Egypt
[e] Department of Geology, Faculty of Science, South Valley University, 83523 Qena, Egypt

ARTICLE INFO

Article history:
Received 8 February 2015
Received in revised form 30 May 2015
Accepted 1 June 2015
Available online 9 June 2015

Keywords:
Facies analysis
Depositional environment
Jurassic
Jubila
Saudi Arabia

ABSTRACT

This article deals with the Upper Jurassic carbonates of the Jubaila Formation, exposed throughout the Tuwaiq Mountains, Central Saudi Arabia and discusses the succession of palaeoenvironments resulting from detailed field and lab work. Based on microfacies analysis and sedimentological data, twelve facies are identified within the Upper Jurassic carbonates at Wadi Hanifa, Central Saudi Arabia. These facies are attributed to six main facies belts. Within these facies and facies belts, four distinct biofacies assemblages are recognized. Deposition took place on an extendable ramp, which probably dipped gently eastwards to the sea. A depositional model relates the identified facies and biofacies to a downdip depositional profile of an inner, middle and outer carbonate ramp. The burrowed lime mudstone and bioclastic wackestone–floatstone of facies belt 1 accumulated in a distal middle ramp to outer ramp. The mollusk-coated grains–intraclast rudstone of facies belt 2 were deposited in the distal middle ramp. The branched stromatoporoids *Cladocoropsis* were deposited in the proximal middle ramp of facies belt 3. The facies of the open lagoon (facies belt 5) and the tidal-flat (facies belt 6) were deposited in the inner ramp behind the ramp crest/shoal facies belt 4. The Early Kimmeridgian Jubaila Formation has been deposited as transgressive and highstand deposits of a third-order depositional sequence, which are mainly controlled by eustatic sea-level changes. During the transgression, an aggradational trend developed, with the construction of a deep subtidal facies of small-scale stacked cycles of mudstones with frequent mottled firm ground and hard ground, storm beds and tempestites. The regressive part has a characteristic progradational trend, with shallow-water carbonate platform deposits arranged into meter-scale coarsening-upward cycles ranged from dolomitic mudstone and wackestone to stromatoporoid packstone and rudstone into bioclastic intraclastic peloidal packstone and grainstone.

1. Introduction

During the Jurassic period the Arabian Plate was tectonically stable and was located at the Equator enabling the development of a wide shallow shelf on the western passive margin of the Neo-Tethys Ocean on which carbonates accumulated over the shelf and inner platform (Al-Saad, 2008). Eustatic sea-level rise combined with intraplate subsidence, led to the development of intrashelf basins on the passive continental margin, including the Gotnia, Arabian, and Rub'Al Khali basins (Al-Husseini, 1997; Ziegler, 2001). In Central Saudi Arabia, Upper Jurassic strata are well exposed and were deposited extensively over the Central Arabian Arch. These strata are the most productive oil reservoirs in the world. They have a significant petroleum potential, and contain an important source, reservoir and seal rocks. Jurassic rocks in Central Saudi Arabia have been described by many authors (Steineke and Bramkamp, 1952; Steineke et al., 1958; Powers et al., 1966; Powers, 1968; Vaslet et al., 1983, 1984, 1991; Manivit et al., 1985a,b, 1986; Enay et al., 1987; Droste, 1990; Le Nindre et al., 1990; Al-Husseini, 1997; Sharland et al., 2001) and several palaeogeographic maps have been published (e.g. Murris, 1980; Al-Husseini, 1997; Ziegler, 2001), based on generalized and sparse

* Corresponding author at: P.O. Box: 2455, Riyadh 11451, Saudi Arabia. Tel.: +966 540325046; fax: +966 14676214.
E-mail addresses: elsorogyabd@yahoo.com, asmohamed@ksu.edu.sa (A.S. El-Sorogy).

http://dx.doi.org/10.1016/j.jafrearsci.2015.06.001
1464-343X/

lithological evidence. The stratigraphy and fossil content have been studied by many authors (e.g. Galal and Kamel, 2004; Hughes, 2004, 2006, 2008; AL-Saad, 2008; El-Sorogy et al., 2014; Youssef and El-Sorogy, 2015; El-Sorogy and Al-Kahtany, 2015).

The present work aimed to describe and interprets the Upper Jurassic strata of the Jubaila Formation Wadi Hanifa, Central Saudi Arabia (Fig. 1) and discusses the palaeoenvironments of the succession resulting from detailed field descriptions and petrographic analysis. The significance of this work comes from the detailed description using facies, facies belts and biofacies assemblages to construct a depositional model for the studied sequence.

2. Materials and methods

Exposures on road-cuts and natural outcrops allowed the analysis of lithofacies, bedding geometries and facies architecture of the Upper Jurassic Jubaila Limestone. Fieldwork was undertaken in 3 main areas on the margins of ravines perpendicular to the depositional dip direction, allowing facies characterization from the shallow-water inner belt to the deeper-water outer belt (see Fig. 1 and descriptions in previous section). Stratigraphic and sedimentological interpretations are based on mapping on outcrop photographs where samples have been located. The sedimentological data gathered included lithology, texture, sedimentary structures, and fossil content. Field observations were complemented

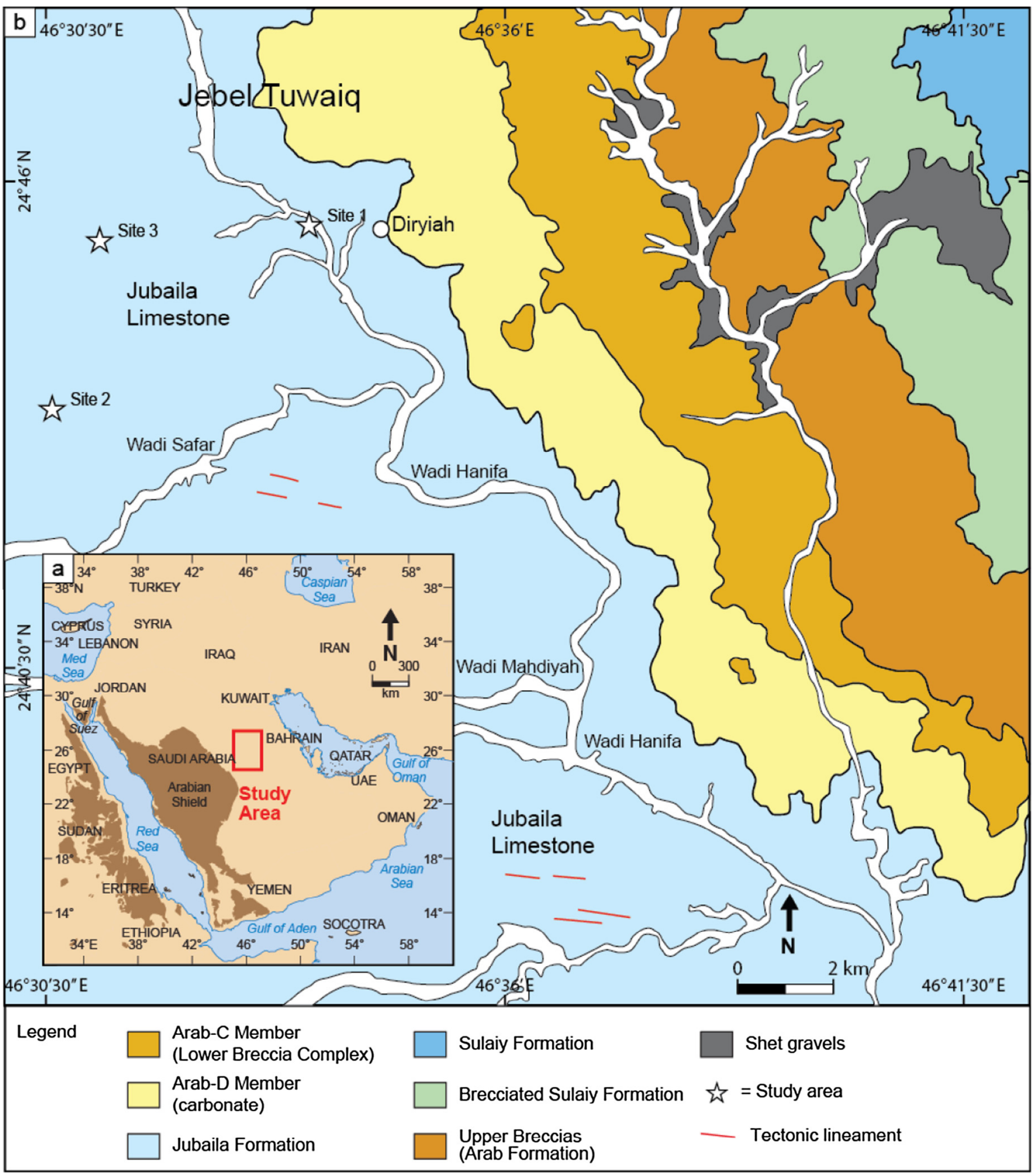

Fig. 1. (a) Regional map of Saudi Arabia. (b) Location map of the study area in Central Saudi Arabia.

with the study of approximately 100 standard thin-sections have been analyzed for their petrographic and diagenetic features, to determine the microfacies which are the basis of the palaeoenvironmental analysis.

100 g of dry samples were soaked in Na_2CO_3 solution, washed over 630, 125 and 63 µm sieves, and then dried in an oven at 60 °C for at least 24 h. The fraction 125–630 µm was investigated qualitatively under binocular stereomicroscope. The foraminifera showed generally poor to moderate preservation in the studied interval. All the representative specimens were mounted on microslides for permanent record and identification. These microslides as well as the SEM-imaged specimens are part of the private collection of the authors; rock samples and residues are deposited in the Department of Geology and Geophysics, College of Science, King Saud University.

3. Geological setting

3.1. Tectono-stratigraphic setting

The present-day Arabian Plate is bordered by different tectonic regimes. The eastern and northern margins of the Arabian Plate are bounded by a compressional plate margin, forming the Zagros Fold Belt (Fig. 2). The northwestern margin is bounded by the Gulf of Aqaba–Dead Sea transform fault system. The southern and western margins are delineated by the Red Sea-Gulf of Aden active rift system (Al-Husseini, 2000; Sharland et al., 2001; Konert et al., 2001).

The Jurassic strata are exposed as a curved belt in the Tuwaiq Mountains of Central Arabian Arch. Central Saudi Arabia is located in the Interior Homocline Platform (stable shelf) (Alsharhan and Kendall, 1986; Alsharhan and Magara, 1995; Fig. 2). Excellent exposures of the Upper Jurassic Jubaila Formation in the Wadi Hanifa provide an ideal example for detailed sedimentological analysis, determining the depositional environments, and hence constructing a detailed depositional model. The Jurassic succession unconformably overlies the Late Triassic Minjur Formation, and is overlain by the Sulaiy Formation of the Berriasian age. It is comprised of, in ascending stratigraphic order, the Marrat, Dhruma, Tuwaiq Mountain, Hanifa, Jubaila, Arab and Hith formations (cf. Hughes, 2004, 2008). These formations are separated by hiatuses of which the duration progressively decreases (Hughes, 2008; Fig. 3). The Jurassic strata consist predominantly of shallow carbonate environments, although evaporitic sediments become more dominant in the Kimmeridgian and Tithonian Arab and Hith formations respectively.

The Upper Jurassic succession consists of the Hanifa, Jubaila, Arab and Hith formations. The Hanifa Formation lies disconformably on the Tuwaiq Mountain Formation and subdivided into two units; a lower muddy carbonate lithofacies of the Hawtah Member (H1) and an upper stromatoporoid and lagoonal carbonate lithofacies of the Ulayyah Member (H2). The Jubaila Limestone lies disconformably upon the Hanifa Formation and consists of moderately deep marine carbonates in the lower part that is overlain by a shallow marine stromatoporoid-associated assemblage. The base of Jubaila Formation was placed at the base

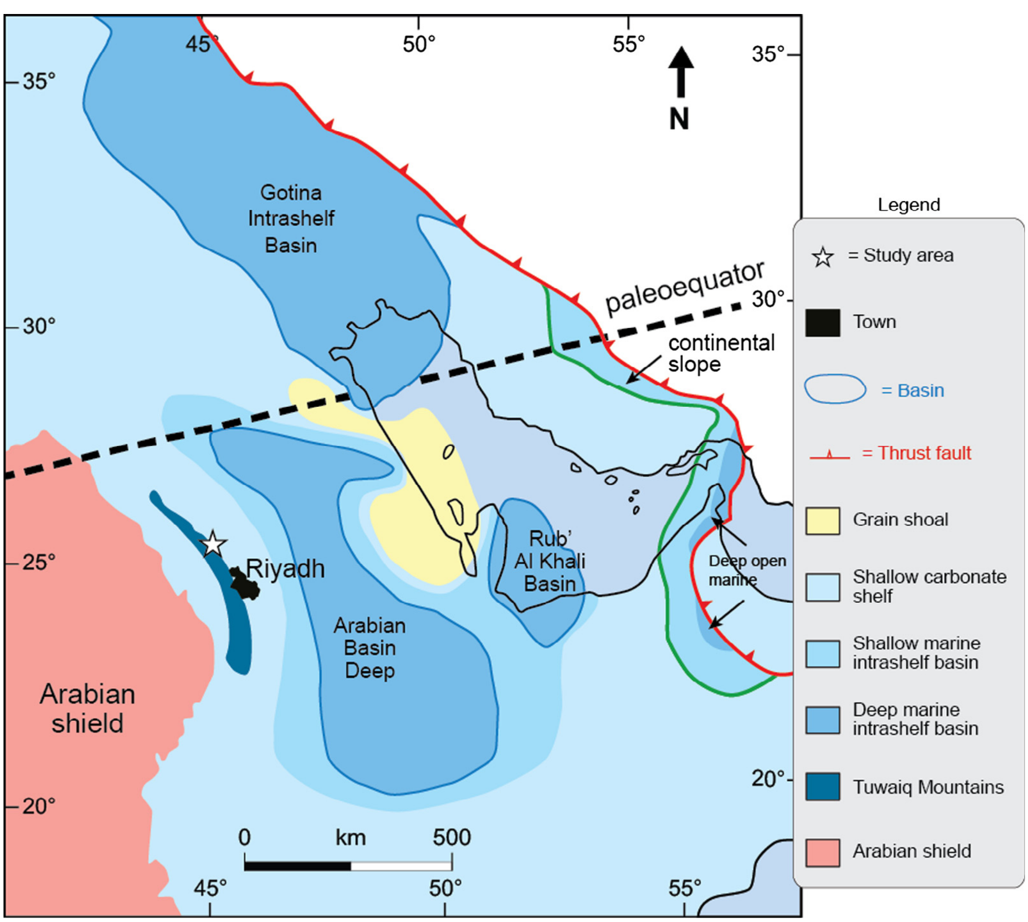

Fig. 2. Late Jurassic (Late Oxfordian-Early Kimmeridgian) Palaeogeographic map of Arabian Peninsula and the surrounding area. Modified from Handford et al. (2002), Al-Husseini (1997), Ayres et al. (1982), Murris (1980).

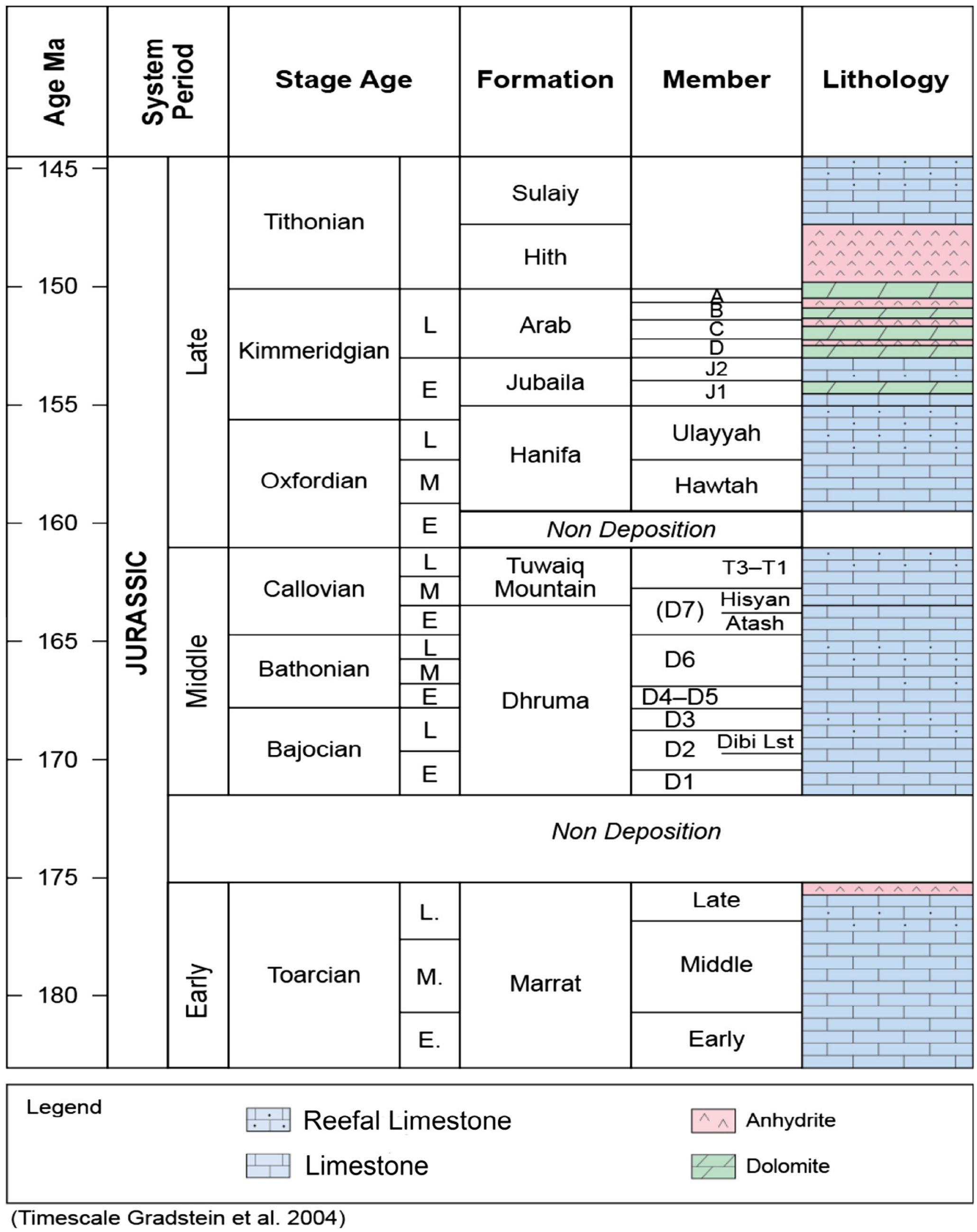

Fig. 3. A generalized stratigraphic column for the Jurassic sediments in Saudi Arabia shows ages, formation and lithology. Modified from Carrigan et al. (1995).

of the reworked Coral-bearing beds that overlie the uppermost Hanifa Formation (cf. Leinfelder et al., 2005). In the outcrop belt, the carbonates pass into sandstones to the south and northwest. It consists of two informal members that include 50 m of the lower J1 and 35 m of the upper J2 member (Enay et al., 1987). Enay et al. (1987) suggested that sediments of the Jubaila Formation were deposited in a lagoon environment. However, the foraminiferal, stromatoporoids, and associated calcareous algal assemblages indicate that the Jubaila Formation was deposited in an extensive and complex, shallow-water-shelf environment, with evidence of high-energy, shoal-water conditions. The presence of benthic foraminifera *Lenticulina* spp., *Nodosaria* spp. along with monaxon and tetraxon sponge spicules, and juvenile costate brachiopods characterizes deposition in moderately deep marine conditions, below the normal fair-weather wave base (Hughes, 2004). The Arab Formation conformably overlies the Jubaila Formation and consists of four stacked carbonate–evaporite cycles, named Arab-D to Arab-A in ascending order. Each cycle starts with subtidal shallow-water carbonates, passing upwards into anhydrite. The Hith anhydrite consists mostly of anhydrite but has an upper carbonate unit, as described by Hughes and Naji (2008).

3.2. Description of the exposures in the Wadi Hanifa

The Jubila Formation exposed on road-cuts at Wadi Hanifa (Fig. 1). A composite vertical succession is compiled in the 3 main areas described below.

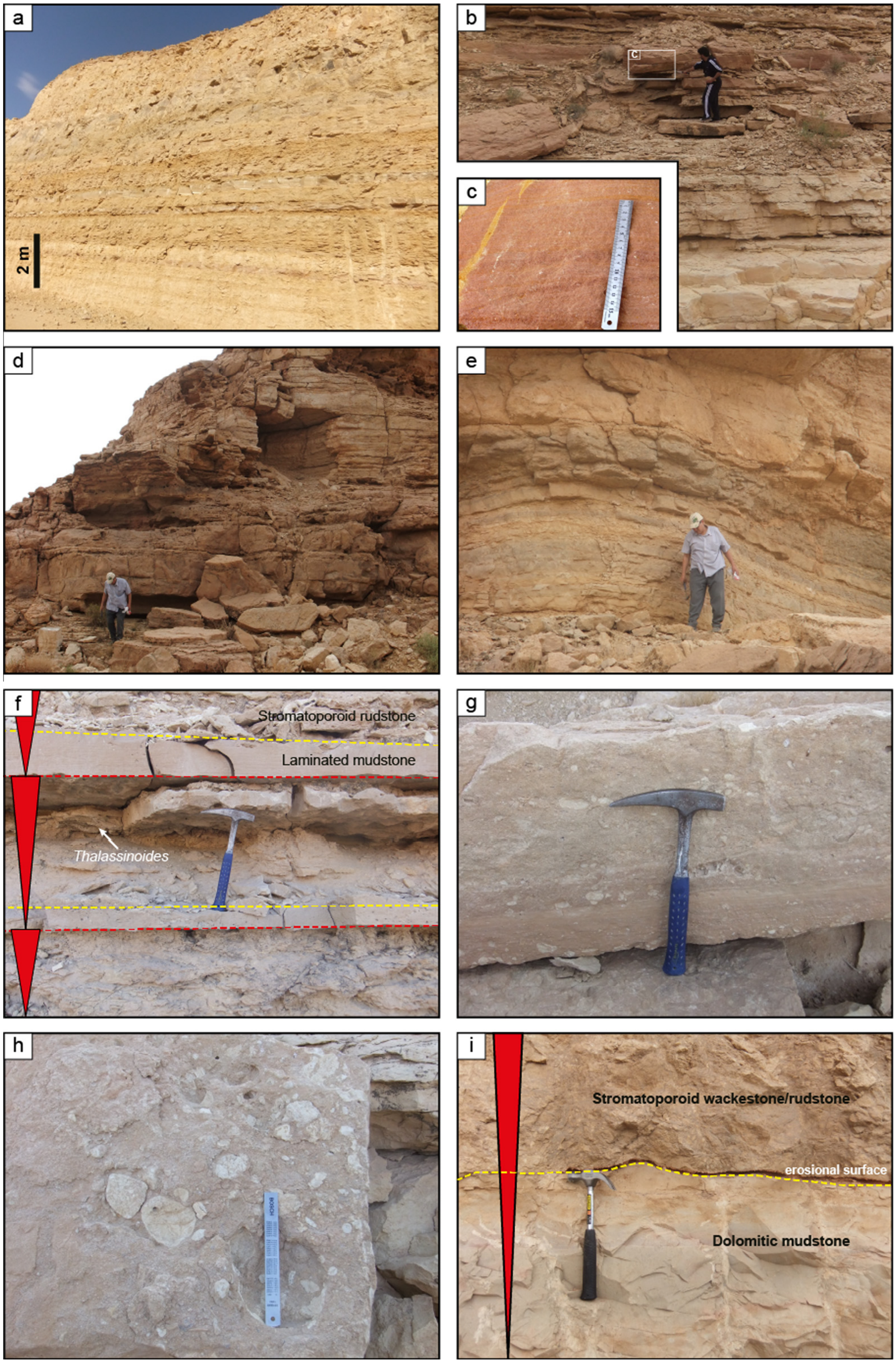

Fig. 4. Field photographs of Jubaila Formation in Central Saudi Arabia. (a) Slightly soft, light-gray to beige calcareous shale, overlain by very hard beige to light gray dolomitized biomicrites grading upward into thickly-bedded reddish dolostone. (b) Medium to thick-bedded reddish dolostone. (c) Close-up view of (b) shows the sandy dolostone facies. (d) Thickly-bedded changes upward to medium-bedded dolostone in medium portions of the Jubaila Formation. (e) Alternations of hard ledges of white to beige limestone and grayish beds of dolostone in the top of the medium portions of the Jubaila Formation. (f) Several shoaling upward high-frequency sequences in the Upper Jubaila Formation, show intensive demarcation on top by the dominant monospecific ichnological suite of *Thalassinoides*. Each cycle starts from dolomitic mudstone and wackestone to stromatoporoid wackestone and packstone into fossiliferous intraclastic peloidal packstone and grainstone. (g) Lag deposits at the contact between mudstone and stromatoporoids in the upper Jubaila Formation. (h) Peloidal–bioclast–intraclast packstone, grainstone, and rudstone of skeletal shoal deposits. (i) Close-up view of shoaling upward high-frequency sequence, where a very coarse stromatoporoid rudstone deposited over the dolomitic mudstone facies with erosive contact. (For interpretation of the references to color in this figure legend, the reader is referred to the web version of this article.)

3.2.1. Site 1 (24° 45′ 23.02″ N, 46° 33′ 11.47″ E)

A compiled section measured as being 10 m composed from the bottom of slightly soft, dark grayish-beige calcareous mudstone, overlain by very hard beige to light gray carbonates grades upward to dolostone (Fig. 4a–c).

3.2.2. Site 2 (24° 43′ 18.73″ N, 46° 29′ 56.68″ E)

A compiled section of 29 m was collected and studied. From bottom to top, it is composed of soft beige calcareous muddy beds in alternations with hard ledges of white to beige limestone and grayish beds of dolostone in the two locations on the top a pinkish color laminated quartzitic limestone is observed (Fig. 4d).

3.2.3. Site 3 (24° 45′ 13.20″ N, 46° 30′ 32.60″ E)

The studied sections at this site represent the major part of Jubila Formation, measured as 43 m in thickness. It is composed mainly, from bottom to top, of white chalky limestone overlain by pinkish quarzitic limestone and alternation of white to beige limestone with grayish dolomitic beds (Fig. 4e–i).

4. Results and discussion

4.1. Biofacies

Semi-quantitative micropalaeontological and macropalaeontological analysis of thin-sections have displayed four distinct biofacies on the basis of vertical distribution of commonly reported species and associated fauna within the Jubaila Formation. The lateral distribution of biofacies exhibits progressing from foraminiferal–spicule, through stromatoporoids (*Cladocoropsis*)–dasyclad algal, foraminiferal-bioclast and foraminiferal biofacies (Fig. 11). The recognition of such biofacies has been helpful in constructing the depositional map for the Upper Jurassic Jubaila Formation. These biofacies assemblages are used as indicators of environmental conditions, mostly related to hydraulic energy levels and paleobathymetry.

4.1.1. Lenticulina-sponge spicule biofacies

4.1.1.1. Description. The *Lenticulina*-spicule assemblage typifies facies F1a and F1b of the FB1 (Table 2). Benthic foraminifera are generally rare and include *Lenticulina muensteri* (Roemer), *Nodosaria* spp., *Alveosepta jaccardi* and agglutinated forms such as *Bigenerina* spp. and the ubiquitous *Kurnubia palastiniensis* (Henson) and *Nautiloculina oolithica* (Mohler). Rare planktonic foraminifers are locally observed. common pelagic crinoid *Saccocoma* present within this biofacies. This foraminiferal assemblage is associated with abundant sponge spicules that include monaxon, triaxon and tetraxon types. The wackestone and floatstone lithofacies are characterized by the presence of faecal pellets of decapod crustaceans *Favreina* sp., brachiopods, few molluskan debris and macrofaunal assemblages. The observed macrofossils include echinoid spines, brachiopods, radiolarians and branched stromatoporoids *Cladocoropsis*.

4.1.1.2. Interpretation. The close associations of the foraminifera *Lenticulina muensteri* (Roemer), *Nodosaria* spp., *Kurnubia palastiniensis* and *Alveosepta jaccardi* with monaxon and tetraxon sponge spicules, Juvenile brachiopods indicate open marine conditions below fair-weather wave base (cf. Hughes, 2006). The local occurrences of planktonic foraminifers may indicate open marine conditions. The pelagic crinoid *Saccocoma* suggest deep environment. The abraded and concentrated nature of the reported fauna implies a general low-energy regime influenced by frequent storms.

4.1.2. Cladocoropsis–dasyclad algae biofacies

4.1.2.1. Description. The *Cladocoropsis*–dasyclad algae assemblage distinguishes facies 3 of the FB3. Abundant branched stromatoporoid *Cladocoropsis mirabilis* (Felix) together with the dasyclad algae (*Clypeina* sp.) and encrusting algal form *Thaumatoporella parvovesiculifera* (Raineri) define this assemblage. This environment was characterized by branched, stratified and domed stromatoporoids such as *Burgundia* spp. (Hughes, 2004). Foraminifera are represented by *Lenticulina* sp., *Nautiloculina oolithica*, miliolids and small-sized planktonic foraminifera. Macrofossils such as brachiopods, echinoid plates, bivalves and echinoid spines and calcareous dinocysts are also present.

4.1.2.2. Interpretation. The *Cladocoropsis*–dasyclad algae is considered to have been deposited in moderately low energy conditions away from breakage by higher wave energy. The common occurrence of grain-rich stromatoporoids *Cladocoropsis* suggests deposition within fair-weather wave base in sheltered proximal middle-ramp (Lindsay et al., 2006). Branched stromatoporoids dominated by *Cladocoropsis mirabilis* are found upslope of the stratified and domal forms (cf. Leinfelder et al., 2005). This palaeoenvironmental interpretation is based on a comparison between distribution of domed and branched corals in the modern environments (James, 1983), where domed stromatoporoids occur in the seaward regions of a bank margin with higher-energy conditions, whereas branched stromatoporoids *Cladocoropsis* occupy

Table 1
Benthic foraminifera, their regional distribution and age range.

No.	Species	Distribution and age range
1	*Palaeogaudryina magharaensis*	Callovian of Sinai (Egypt); Oxfordian of Syria, Oxfordian-Kimmeridgian of Saudi Arabia
2	*Kurnubia wellingsi*	Oxfordian of eastern Mediterranean, Italy and France, lower Oxfordian of Syria and Callovian to Oxfordian of Saudi Arabia
3	*Kurnubia jurassica*	Neocomian of France, Italy, eastern Mediterranean; Barremian to lower Aptian of Syria and Callovian of Saudi Arabia
4	*Pfenderina neocomiensis*	Middle Jurassic of Saudi Arabia and the Middle East
5	*Kurbubia palastiniensis*	Callovian, Oxfordian of Palestine, Syria, Saudi Arabia, France, Morocco, Iraq and former Yugoslavia
6	*Haurania deserta*	Saudi Arabia, Iraq, Morocco, Turkey, and Italy
7	*Choffatella decipiens*	Saudi Arabia, Syria, Lebanon and Morocco
8	*Nautiloculina oolithica*	Jurassic to Lower Cretaceous of Europe, eastern Mediterranean; Callovian to Tithonian, Barremian to lower Aptian of Syria, Jurassic of Saudi Arabia
9	*Lenticulina muensteri*	Middle Jurassic of the Middle East
10	*Nautiloculina circularis*	Middle Jurassic of Saudi Arabia and Middle East
11	*Oolina globosa*	Middle Jurassic of Central Saudi Arabia
12	*Evolutinella* sp.	Middle Jurassic of Central Saudi Arabia

The distribution after: Kuznetsova et al. (1996).

Table 2
Summary of characteristics and distribution of carbonate lithofacies, and depositional setting in the Upper Jurassic Jubaila Formation.

Facies Belt	Facies	Components	Sedimentary structures	Pore Type	Depositional Environment
Distal Middle-ramp to Outer-ramp Environment (FB1, Fig. 5)					
1	Burrowed lime mudstone–wackestone facies (F1a)	Bioclasts are scarce include forams, sponge spicules, *Saccocoma*, Faecal pellets *Favreina* sp., Juvenile brachiopods, and few molluskan debris. Few echinoid spines, brachiopods, radiolarians, *Cladocoropsis*, bivalve *Bositrabuchi* and intraclasts	Massive and characterized by horizontal *Planolites* burrows. Capped by *Thalassinoides*-burrowed firm grounds. High-energy debris facies with tempestites	Microporosity and moldic	Deep, open marine conditions below the wave base
2	Bioclastic floatstone to wackestone facies (F1b)	Bioclasts include forams, mollusks, brachiopods, *Cladocoropsis* and echinoid plates Non-skeletal components include micritized grains and few quartz grains	No sedimentary structures	Microporosity and moldic	Low-energy regime influenced by frequent storms
Distal Middle-ramp Environment (FB2, Fig. 6)					
3	Mollusk-coated grain–intraclast sandy rudstone facies (F2)	Sheet-like geometry of rudstones, grainstone, and mud-rich packstone textures. Bioclasts are gravel-size, poorly sorted clasts of bivalves, gastropods, coated grains, intraclasts, micritized grains, brachiopod shells, brachiopod spines, oncoids, coral fragments, *Cladocoropsis mirabilis* and forams	No discernible sedimentary structures	Interparticle, moldic, and intraparticle	Storm-induced high-energy debris flows that transported debris and matrix downslope into the distal middle-ramp environment, slightly beyond the barrier shoal
Proximal Middle-ramp Environment (FB3, Fig. 7)					
4	*Cladocoropsis*-intraclast–peloidal–bioclasticpackstone-grainstonefacies (F3)	Burrowed, heterogeneous, muddy sediments containing abundant abraded and sorted *Cladocoropsis* Other bioclasts include domal stromatoporoids, dasyclad algae, brachiopods, echinoid plates, bivalves and echinoid spines The non-skeletal grains contain reworked intraclasts, peloids, detrital quartz grains and glauconite pellets	Vague cross-stratification structures oriented toward the platform margin	Interparticle and large fenestral voids	Open marine, normal salinity proximal middle-ramp environment, with deposition within fair-weather wave base
Ramp-crest Shoal Environment (FB4, Fig. 8)					
5	Foram-bioclast–oncoid grainstone/rudstone facies (F4a)	Coarse-grained, well-sorted and contains grainstone and rudstone textures. Whole and fragmented bioclasts including forams, dasyclad algae, brachiopods, stromatoporoids, bivalves and faecal pellets *Favreina* sp. Agglutinated forams *Rhaxella*. Non-skeletal grains contain oncoids, intraclasts, micritized grains and detrital quartz grains	Planar cross-bedding and cross-lamination structures	Interparticle and intraparticle	High-energy waning flows associated with storms. Facies (F4a) is interpreted to have been deposited in the ramp-crest sand shoal environment
6	Foram-bioclast-peloidal packstone/grainstone facies (F4b)	Small, sub-rounded, moderately well sorted, spherical to irregular grains with no internal structure Bioclasts include forams, dasyclad algae, *Cladocoropsis mirabilis*, brachiopods and bivalves. Fine-grained, subrounded to rounded quartz grains are common	Planar and low-angle cross-lamination	Interparticle, Moldic and intraparticle	Shallow-water high- to moderate-energy conditions based on the mature to moderately mature texture and the faint planar cross bedding and cross lamination. A central to fore-shoal environment
Inner-ramp Environment (FB5, Fig. 9)					
7	Peloidal packstone/grainstone facies (F5a)	Small to medium, sub-rounded, poorly sorted, spherical to irregular peloids. Bioclasts are scarce and restricted to forams, dasyclad algae, echinoid spine and few molluskan debris The non-skeletal fraction include micritized grains, small-sized intraclasts and fine to medium grade, subrounded to rounded quartz grains	Massive	Interparticle	Shallow platform interiors comprising restricted inner-ramp lagoonal environments with moderate water circulation
8	Laminated dolomitized peloidal packstone (F5b)	Compacted, ellipsoidal, flattened and unevenly distributed mud peloids and microbial peloids associated with bivalve and echinoid plates.	Laminated with burrows	Interparticle	Quiet, shallow-water, protected inner ramp lagoonal environments

Table 2 (*continued*)

Facies Belt	Facies	Components	Sedimentary structures	Pore Type	Depositional Environment
9	Burrowed bioclastic wackestone/ floatstone facies (F5c)	Matrix supported, fine-grained facies and massive beds. Bioturbation occurs as horizontal burrows infilled with fine to coarse quartz sand. Skeletal grains are typically dominated by bivalve fragments, forams, dasyclad algae, brachiopods, *Cladocoropsis*, echinoid spines, ostracods and faecal pellets *Favreina* sp. The non-skeletal grains contain peloids, detrital subrounded quartz grains and lithoclasts	Massive beds with horizontal burrows	None	A less-restricted lagoon under relatively higher energy and shallower conditions, which influenced by frequent storm events
10	Peloidal bioclastic packstone/floatstone (F5d)	Large scale bioclasts distributed throughout the sediment forming the floatstone texture. Bioclasts include forams, dasyclad algae, bivalves, cerithid gastropods, and corals. Non-skeletal grains consist of small, sub-rounded, moderately well sorted, and spherical to irregular peloids. Low proportions of scattered oncoids and intraclasts in this facies	Not observed	Interparticle and moldic	Restricted lagoon
Tidal flat Environment (FB6, Fig. 10a)					
11	Dolomitized mudstone (F6a)	Medium grained (50–160 μm), euhedral rhombs float in the carbonate mud matrix	Not observed	None	Tidal flat with normal or slightly elevated salinity
12	Breccia (F6b)	Light gray and beige, monomict to polymict, poorly sorted, angular to subangular dololaminite mudstone, dedolomites, evaporite pseudomorphs	Not observed	None	Low-energy restricted environment/ evaporate collapse-related breccia (?)
Diagenetic facies					
13	Dolomite	Dolomite rocks ranging from a slightly dolomitized single bed to completely dolomitized rock of meters-thick. Replacive, medium grained (50–100 μm), euhedral to subhedral dolomite rhombs replacing the matrix and grain components	Not observed	None	Seepage-reflux dolomitization in shallow burial
Diagenetic facies					
14	Dedolomite	Fine to medium crystalline (mostly between 30 and 130 μm) and subhedral to anhedral	Not observed	None	Vadose diagenesis and dissolution by meteoric water during prolonged subaerial exposure

lower energy, sheltered sites on the leeward side of the stromatoporoid bank.

4.1.3. Foraminiferal-bioclastbiofacies

4.1.3.1. Description. This assemblage characterizes facies F4a of the FB4. Biofacies 3 (Fig. 12: 1–12) consists of a combination of most of the biofacies described for biofacies 4, but accompanied by dasyclad algae, brachiopods, branched stromatoporoids, bivalves and faecal pellets of decapod crustaceans *Favreina* sp. and non-skeletal grains. Foraminifera consists of diverse assemblage of robust (*Nautiloculina oolithica*, *Kurnubia palastiniensis* and *Mangashtia vienotti*), calcareous *Lenticulina* spp. and agglutinated forms.

4.1.3.2. Interpretation. The well-sorted and often over packed foraminifera and dominance of planar cross-bedding structure indicate higher-energy depositional environment. The abraded skeletal detritus such as branched stromatoporoids *Cladocoropsis mirabilis* and foraminifera *Lenticulina* spp. indicate transport by wave and storm events under shallow and agitated conditions.

4.1.4. Foraminiferal biofacies

4.1.4.1. Description. The foraminifera assemblage represents facies F5c, F5d of the FB5 (Fig. 13). This assemblage is characterized by high foraminiferal species diversity (Table 1). Benthic foraminifera are dominated by *Kurnubia palastiniensis* (Henson), *Nautiloculina oolithica* (Mohler) *Redmondoides lugeoni* (Redmond), *Alveosepta jaccardi* (Schrodt), *Pfenderina neocomiensis* (Pfender) and miliolids. Other bioclasts are scarce and dominated by bivalve fragments, dasyclad algae, brachiopods, echinoid spines, ostracods and faecal pellets of decapod crustaceans *Favreina* sp. branched stromatoporoids *Cladocoropsis* and dasyclad algae are rarely present. The occurrence of quartz grains indicates proximity to a source of terrestrially-derived sediment.

4.1.4.2. Interpretation. Despite the *Kurnubia palastiniensis* and *Nautiloculina oolithica* are of limited palaeoenvironmental importance because they were recorded in the most biofacies of Jubaila Formation (Hughes, 2008). The robust *Kurnubia palastiniensis* and *Nautiloculina oolithica* along with *Alveosepta jaccardi*, *Pfenderina neocomiensis* and miliolids indicate deposition in an inner shelf, shallow-water lagoon to a back bank environment. The larger

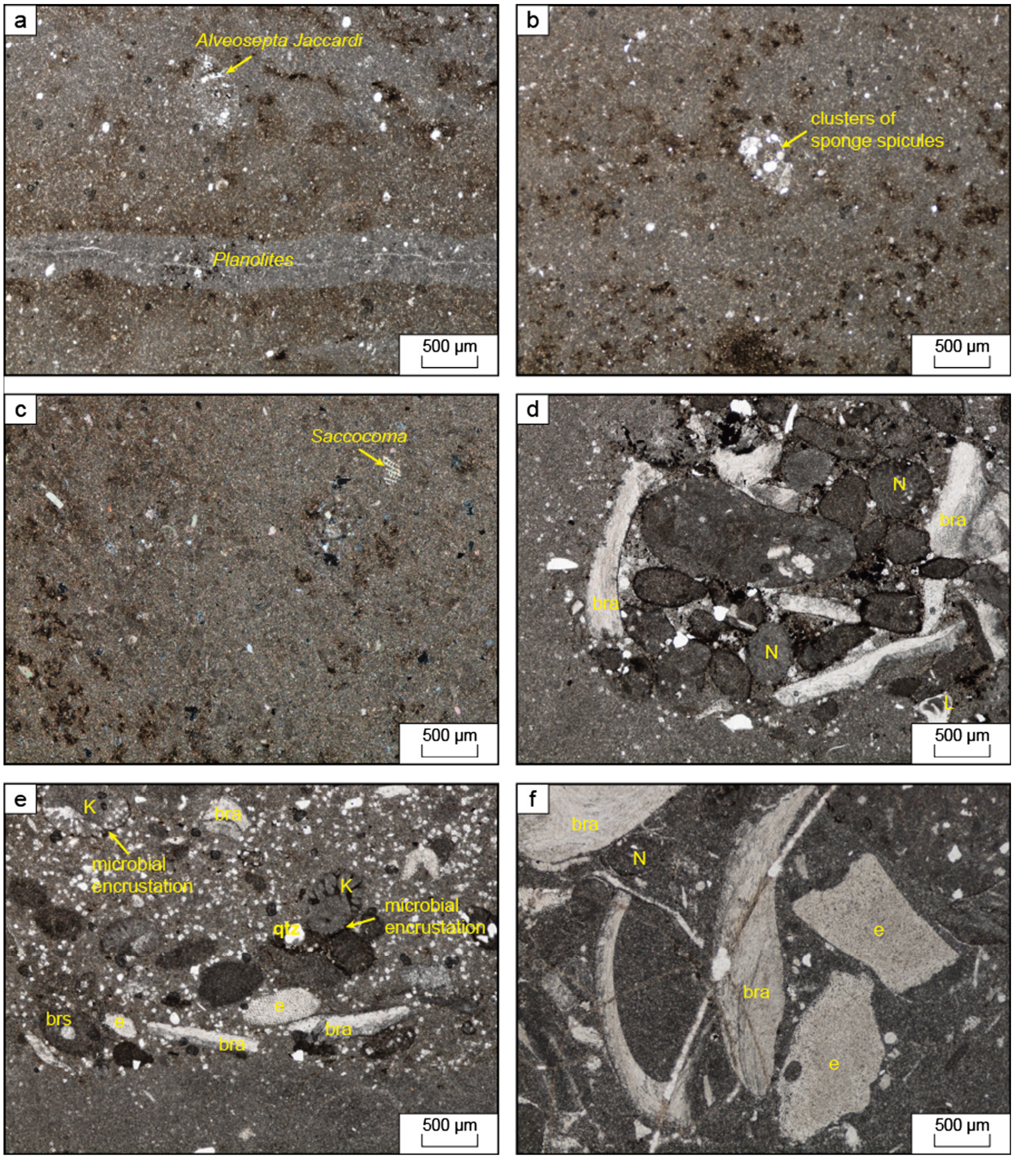

Fig. 5. Optical photomicrograph (PPL) of the distal middle-outer ramp facies belt (FB1). (a) Burrowed lime mudstone–wackestone facies (F1a), with scarce bioclasts include benthic foraminifera (*Alveosepta jaccardi*) and monaxon sponge spicules. (b) Cluster of sponge spicules embedded in the bioturbated mud matrix. (c) Bioturbated mudstone contains scarce pelagic crinoids *Saccocoma*. (d) Bioclastic floatstone to wackestone facies (F1b) consists of medium- to coarse-grained disorganized bioclasts and micritized grains floating in the muddy matrix. Bioclasts include *Nautiloculina oolithica* (N), *Lenticulina* (L), brachiopods (bra). (e) Concentration of brachiopod shells (bra), brachiopod spine (brs), forams *Kurnubia palastiniensis* (K), *Lenticulina* (L) and echinoids (e) result from non-cohesive debris flow in the middle-ramp setting. The bioerosion, abrasion and encrustation prove transport. Note that fine-crystalline dolomite rhombs and few quartz grains (qtz) are embedded in the mud matrix. (f) Brachiopod (bra) and echinoid (e) fragments are embedded within a bioclastic wackestone matrix contains a fine reworked foraminifera *Nautiloculina oolithica* (N).

agglutinated textulariids foraminifera *Redmondoides lugeoni* indicated deposition in the inner platform. The associations of (cerithid) gastropods, ostracods, benthic foraminifera and bivalve indicate intertidal environments, where low diversity organisms that adapted to rapidly changing stress conditions.

4.2. Facies analysis and depositional environment

Twelve carbonate facies are defined within the Upper Jurassic Jubaila Formation using the key features such as sediment color, bed thickness, bedding geometry, grain components, sedimentary texture, sedimentary structures, pore types, fossil content, and identified ichnofacies. Diagenetic facies (medium-crystalline dolomites and dedolomites) that frequently destroy evidence of original depositional lithofacies are locally recorded. Petrographic investigation included description of grain types, and texture in order to determine the depositional facies and early diagenetic features. Distinctions between the carbonate facies are determined by the textural classification of Dunham (1962), as modified by Embry and Klovan (1971), and abundant biotic assemblages. Table 2 summarizes the sedimentological characteristics and a brief interpretation of the depositional environments of the defined facies.

The succession shows no evidence of slope deposits, suggesting that the Jubaila Formation was deposited on storm-influenced homoclinal ramp, as described by Read (1982, 1985, 1989), Tucker and Wright (1990), Burchette and Wright (1992), Jones and Desrochers (1992), Wright and Burchette (1996) and Flügel (2004). The distal mid-ramp to outer-ramp (Fig. 5) and the progressive decrease of wave energy in the mid-ramp areas is reflected by the decrease of burrowed lime mudstone–wackestone

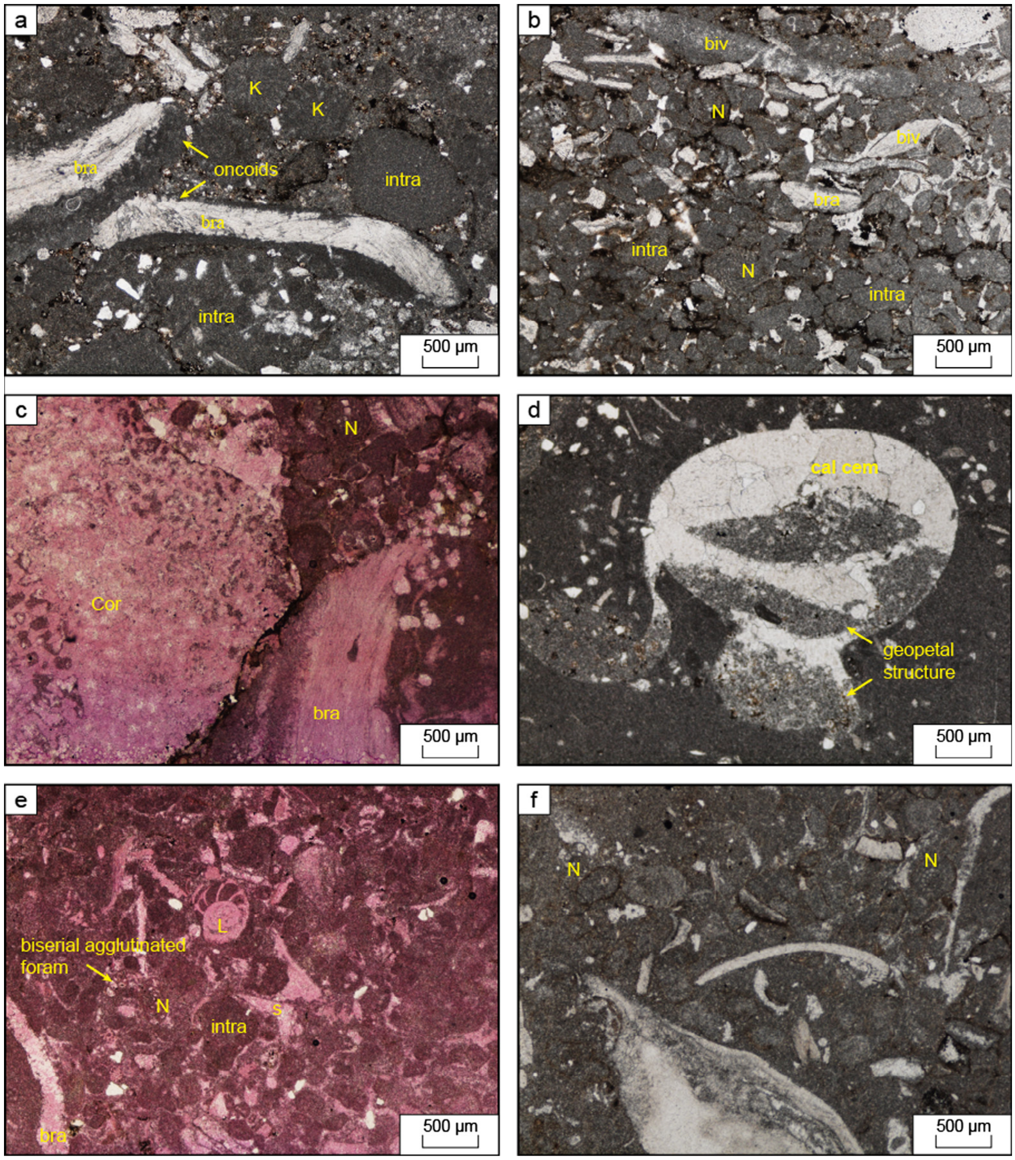

Fig. 6. Optical photomicrograph (PPL) of the distal middle-ramp facies belt (FB2). (a) Mollusk-coated grain–intraclast sandy rudstone facies (F2) composed of gravel-sized oncoids formed by microbial encrusting brachiopod shells (bra), micritized *Kurnubia palastiniensis* (K) and intraclasts (intra). (b) Highly compacted, elongated gravel-size intraclasts (intra), brachiopods (bra), bivalves (biv) and *Nautiloculina oolithica* (N). (c) Highly dissolved aragonitic coral fragment (Cor) is preserved as molds that partially filled with internal sediments and coral debris and brachiopod (bra). (d) Aragonitic brachiopod shell shows geopetal structure that consists of internal sediments that filled with sparry calcite cement (calcem). (e) Bioclastic sands form packstone texture that contain peloids, small biserial agglutinated foraminifera, *Nautiloculina oolithica* (N), *Lenticulina* (L), sponge spicules (S), brachiopod shells (bra) and intraclasts (intra). (f) Intraclasts contain reworked foraminifera *Nautiloculina oolithica* (N) indicate that storm-induced high-energy debris flows that transported debris and matrix down slope into the distal middle-ramp environment.

facies (F1a) and bioclastic floatstone to wackestone facies (F1b). The distal middle-ramp (Fig. 6) is characterized by the mollusk-coated grains–intraclast sandy rudstone (F2). The proximal middle-ramp (Fig. 7) is represented by the *Cladocoropsis* -intra clast–peloidal–bioclastic limestone facies (F3). The ramp-crest shoal environment (Fig. 8) includes foram-bioclast–oncoid grainstone/rudstone facies (F4a) and foram-bioclast-peloidal packstone/grainstone facies (F4b). The inner carbonate ramp (Fig. 9) is characterized by the presence of a low-energy lagoonal environment, which includes peloidal packstone/grainstone facies (F5a), laminated dolomitized peloidal packstone (F5b), burrowed bioclastic wackestone/floatstone facies (F5c), and peloidal bioclastic packstone/floatstone (F5d). The tidal-flat environment (Fig. 10a) is represented by dolomitized mudstone facies (F6). These facies are grouped into six facies belts showing different sub-environments and numbered from proximal to distal positions (inner to mid to outer ramp) with distinctive sub- and micro-facies (Figs. 11 and 12). Diagenetic facies were suggested to include the most important diagenetic features; dolomite and dedolomite facies.

4.3. Diagenetic facies

4.3.1. Description

4.3.1.1. Dolomite facies. Dolomite rocks occur in different stages of development, ranging from a slightly dolomitized single bed to completely dolomitized rock of meters-thick. The dolomite interval is easily recognized in the outcrop as it tends to be harder and have

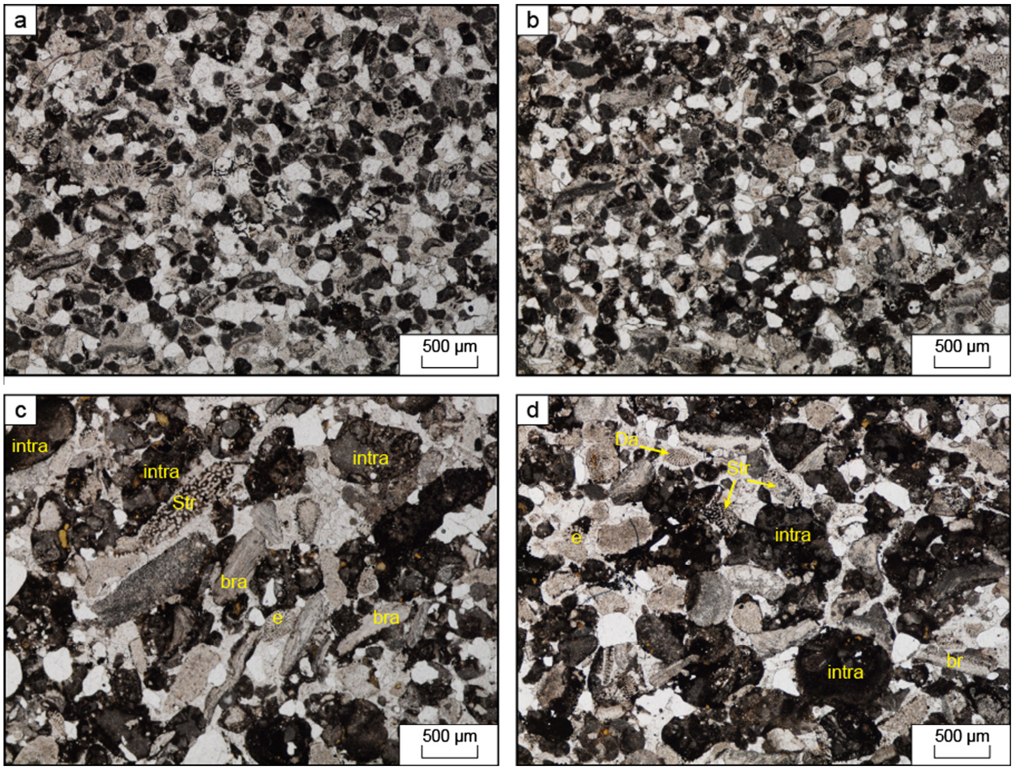

Fig. 7. Optical photomicrograph (PPL) of the proximal middle-ramp facies belt (FB3). (a) *Cladocoropsis*-intraclast–peloidal–bioclastic limestone facies (F3) consists of branched stromatoporoids (*Cladocoropsis mirabilis*) with a packstone matrix contains interparticle porosity. (b) Abundant abraded and sorted *Cladocoropsis*, intraclasts and peloids in heterogeneous, muddy sediments and sparry calcite cement fill the interparticle porosity. (c) *Cladocoropsis*-bioclastic rudstone exhibits vague cross-stratification structure and composed of stromatoporoids *Cladocoropsis* (str), intraclasts (intra), brachiopods (bra) and echinoids (e). (d) Intraclast–bioclast grainstone, with mottled intraclasts (intra), stromatoporoids *Cladocoropsis* (str), dasyclad algae (Da) and echinoids (e).

a darker color (rusty brown with reddish hues) than the overlying and underlying cream to yellow limestone (Fig. 10b). These dolomites are replacive, medium grained (50–100 μm), euhedral to subhedral dolomite rhombs replacing the matrix and grain components (Fig. 10c). Matrix-replacive dolomite is the most common type of dolomite by volume in the Upper Jurassic Jubaila Formation may be a result of burial dolomitization. Intensity of dolomitization varies from isolated rhombs floating in the matrix (Fig. 10d) to idiotopic and hypidiotopic fabric-destructive mosaic textures (Fig. 10c). The fabric-destructive dolomite is generally rare to absent in the lower open-marine facies but common in the more restricted facies of the Jubaila Formation. An open mosaic of rhombs gives rise to a high intercrystalline porosity that filled with blocky calcite cement (Fig. 10c). The fully dolomitized intervals are characterized by two textural populations with different crystal sizes and shapes, and degrees of pore interconnections. Fabric-destructive dolomite almost completely obliterates the precursor limestone texture and leaves only ghosts of the original grains. This dolomite consist of medium- to coarsely crystalline (50–100 μm), euhedral to subhedral rhombs that have replaced much of the primary depositional fabric. These dolomite crystals also show zoning pattern under transmitted light with alternating cloudy centers "inclusions-rich" and clear limpid rims "inclusions-free". A replacive, fine to medium grained (20 μm), predominantly subhedral dolomite occurs in patches of burrow-like fabric (Fig. 10e). Considering the various inclusions and the partially filled character of dolomitized patches, burrow-filling dolomite seems to replace a precursor burrow fill. The two-population texture are most likely to be result from the textural differences have been originally inherited from the precursor limestone. Microfacies at the diffuse lower contact frequently reflects (highly) restricted lagoonal environments. Higher up in the dolomite beds, dolomitization is usually fabric-destructive, so that in some cases no microfacies features of the precursor rock are preserved. In the uppermost part of a dolomite cap, leaching may occur.

4.3.1.2. Dedolomite facies. The dedolomites commonly occurs in the upper part of the Jubaila Formation in the study area. These rocks are creamy to light brown in hand specimen, where recrystallization commonly follows bed geometries and the upper surfaces show prominent dissolution vugs. In thin section, the dedolomites are fine to medium crystalline (mostly between 30 and 130 μm) and subhedral to anhedral (Fig. 10f). These dedolomites resemble the "hollow dolomites" described by Swart et al. (2005), Jones (2007), and Nader et al. (2008). Most rhombs are corroded and one or more of their corners are missing. The dedolomites show clear rims and enclose relicts of the precursor dolomite crystals (Fig. 10g). Continuous replacement of dolomite by calcite via dissolution/precipitation is indicated by xenotopic fabrics. Calcite pseudomorphs are interpreted to postdate the former xenotopic dolomite, consisting of sparite with widely varying crystal diameters.

4.3.2. Interpretation

Dolomitization of the subtidal and shoal sediments of the Jubaila Formation is suggested to occur according to the seepage reflux model based on their petrographic characteristics and stratal geometries. The seepage-reflux model was originally proposed by Adams and Rhodes (1960) to explain dolomitization by dense hypersaline brines derived from the back reef evaporite lagoon refluxed into underlying sediments. Recent research on

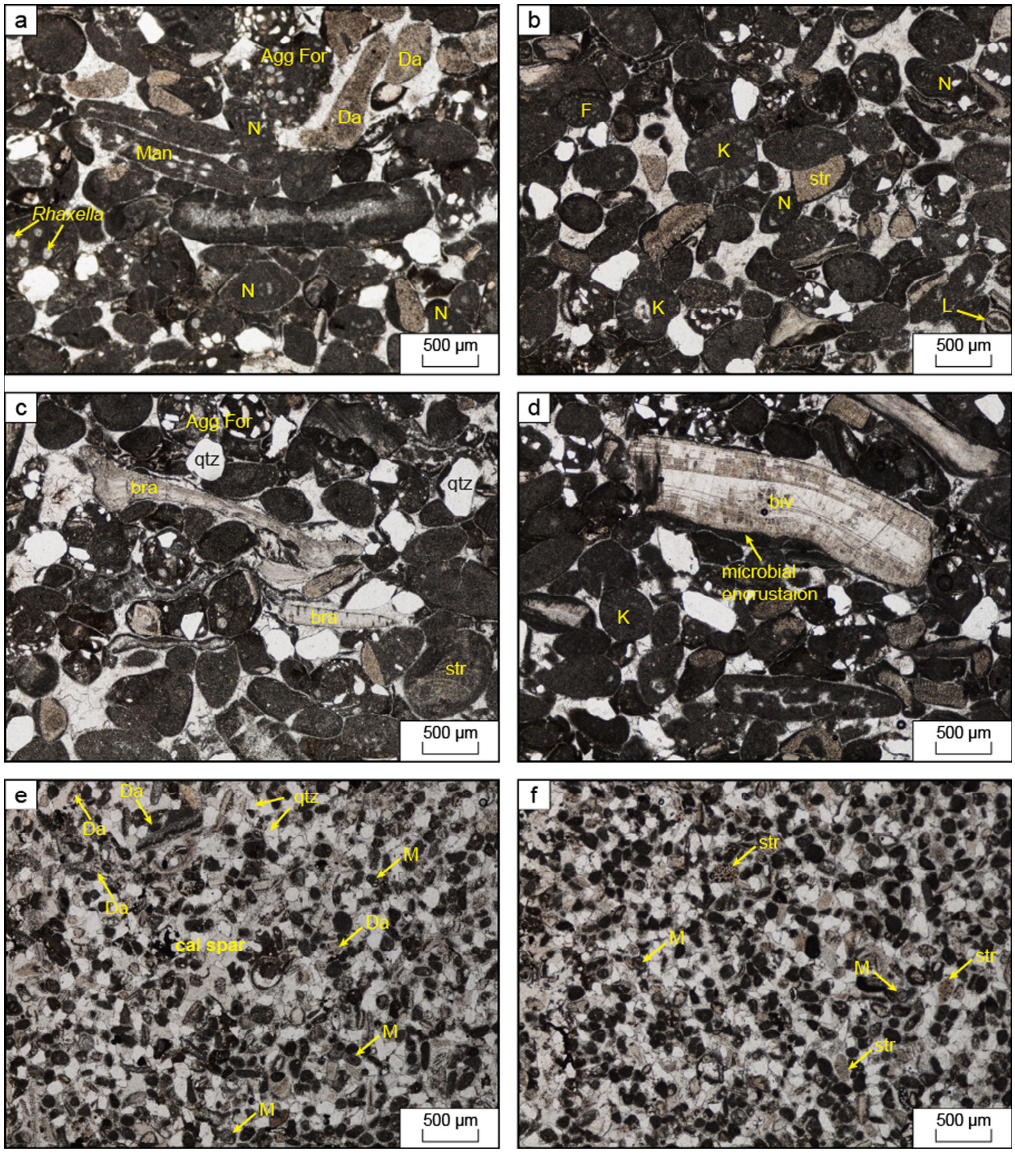

Fig. 8. Optical photomicrograph (PPL) of the ramp-crest shoal facies belt (FB4). (a) Foram-bioclast–oncoid grainstone/rudstone facies (F4a) composed of cross-bedded, intraclast–peloid-coated grain-ooid grainstone with abundant interparticle porosity. (b) *Kurnubia palastiniensis* (K), *Nautiloculina oolithica* (N), *Lenticulina* (L) and faecal pellets *Favreina* sp. (F) in sparry calcite cement. (c) Oncoid-bioclastic grainstone, with agglutinated foraminifera (aggfora), brachiopods (bra) and quartz grains (qtz). (d) The grainstone is cemented by isopachous fringe of submarine fibrous calcite. Note: the bivalve shell fragment coated by microbial encrustations. (e) Foram-bioclast-peloidal packstone/grainstone facies (F4b) composed of small, sub-rounded, moderately well sorted, and spherical to irregular peloids with miliolids (M) and dasyclad algae (Da). (f) Peloids, Miliolid forams (M), dasyclad algae, branched stromatoporoids *Cladocoropsis* (str), brachiopods (bra) and bivalves in sparry calcite cement completely fill the interparticle porosity.

seepage-reflux dolomitization emphasizes the role of mesohaline brines (cf. Qing et al., 2001; Melim and Scholle, 2002).

The restricted lagoonal facies, which lie above the open-marine shelf facies, could be an alternative source of refluxing brines. These transitional facies are characterized by a lack of normal marine fauna, a dominance of restricted-marine peritidal carbonate facies, evaporite pseudomorphs and a restricted-marine fauna, i.e. dwarf mollusks and agglutinated benthic foraminifera suggesting waters of elevated salinity. However, the absence of massive evaporites, and/or evaporite collapse breccias, suggest that only mesohaline brines were presented during the deposition of the inner ramp (i.e. below the gypsum saturation level of 120‰ salinity). During low stands, the water recharge from the open sea had possibly become progressively restricted by shoal barrier. However, the complete isolation of the system did not occur as indicated by the absence of massive evaporite deposits. The salinity of waters present within the inner ramp restricted lagoon sediments most probably became elevated enough to create brines of a sufficient density to start a reflux flow.

The geometric distribution of dedolomites in the upper part of the studied carbonates suggests that massive influx of fluids (e.g. meteoric) was the driving mechanism for dedolomitization. The petrographic features of dedolomite, suggest only that chemical resetting. Therefore, the dedolomitization had most probably resulted from vadose diagenesis and dissolution during prolonged subaerial exposure. An alternative explanation would be alteration of unstable ferroan dolomite by oxygenated meteoric water (Al-Hashimi and Hemingway, 1973; Purser et al., 1994). This would result in the liberation of Fe^{2+} and ferric iron precipitation, which gives the rock its characteristic brown to red color.

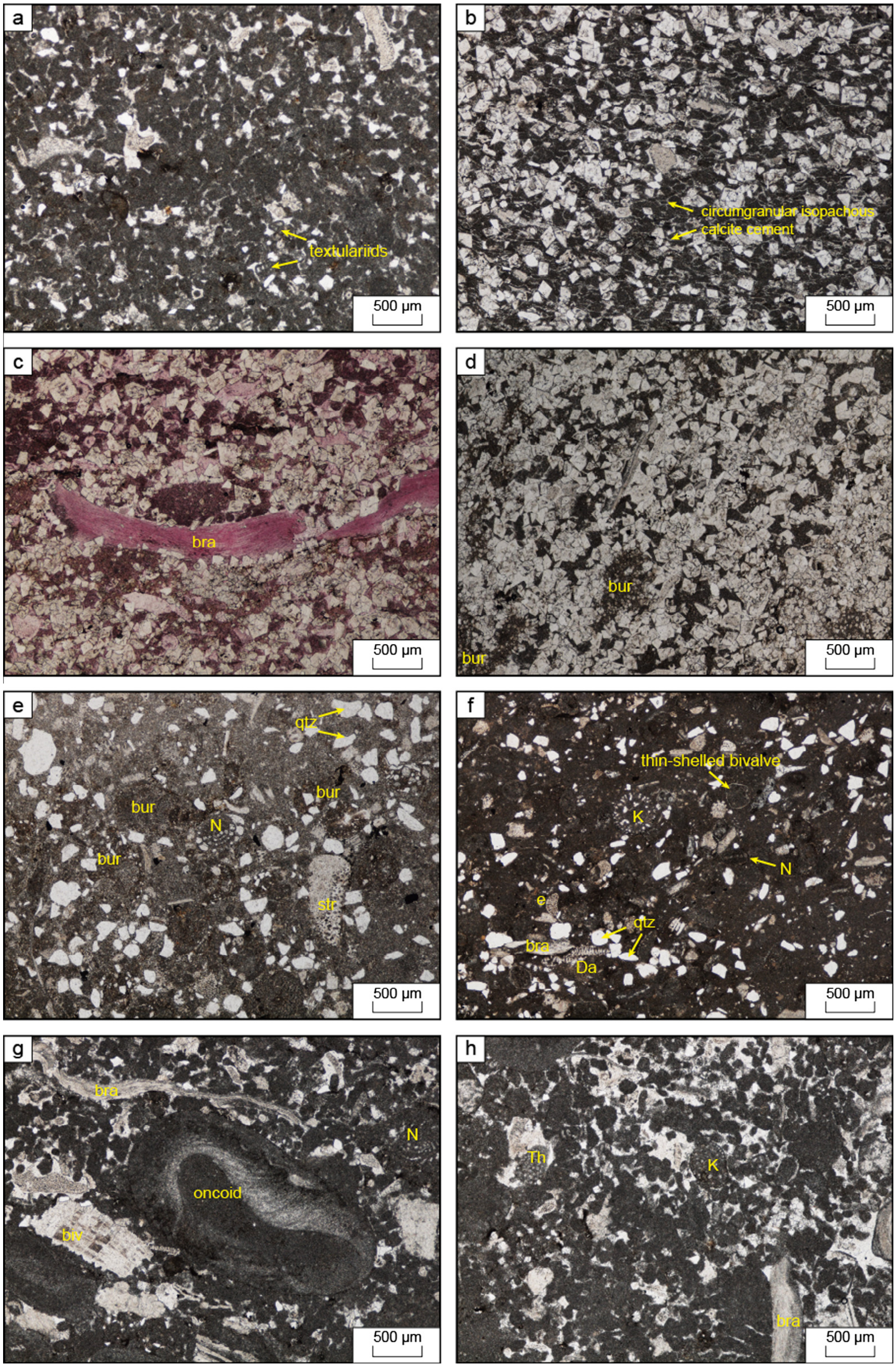

Fig. 9. Optical photomicrograph (PPL) of the inner-ramp facies belt (FB5). (a) Peloidal packstone/grainstone facies (F5a) with few textulariid forams. (b) Laminated dolomitized peloidal packstone facies (F5b) composed of compacted, ellipsoidal, flattened mud peloids cemented by thin circumgranular fine isopachous calcite. (c) Medium-grained dolomite rhombs replace peloids and brachiopod shells (bra). (d) Burrows in peloidal packstone facies are easily distinguished by difference in color, texture and differential dolomitization. (e) Burrowed bioclastic wackestone/floatstone facies (F5c), with *Nautiloculina oolithica* (N) and branched stromatoporoid *Cladocoropsis* embedded in micritic matrix. (f) *Kurnubia palastiniensis* (K), *Nautiloculina oolithica* (N), echinoids (e), dasyclad algae (Da), thin-shelled bivalves and brachiopods (bra) in micritic matrix enriched with quartz grains (qtz). (g) Peloidal bioclastic packstone/floatstone (F5d), with oncoids, brachiopods (bra) and bivalves (biv) embedded in peloidal packstone. (h) *Kurnubia palastiniensis* (K), Dasyclad algae *Thaumatoporella parvovesiculifera* and faecal pellets of decapod crustaceans *Favreina* sp. (F) and brachiopods (bra) in peloidal packstone.

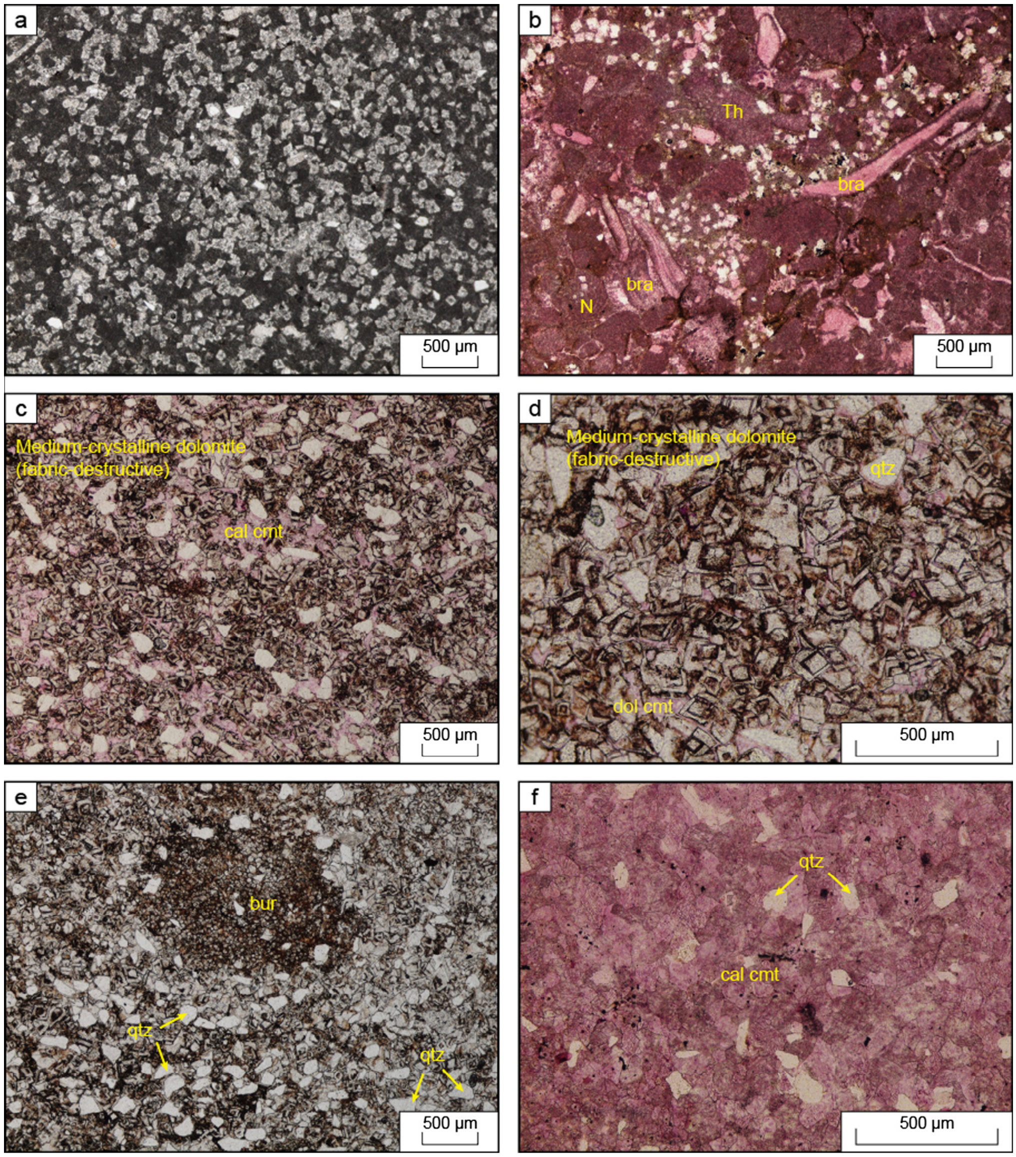

Fig. 10. Optical photomicrograph (PPL) of the diagenetic facies. (a) Small-grained, subhedral dolomite rhombs that are always associated with tidal flat environment. (b) Photomicrograph (PPL) of a stained thin-section showing few dolomite crystals float in muddy matrix of the bioclastic packstone lithofacies. (c) Medium-grained, idiotopic dolomite (“floating/packed rhoms”), commonly with zoned crystals. (d) Close-up view of the medium-grained dolomite crystals showing cloudy centers “inclusions-rich” and clear limpid rims “inclusions-free”. Note the sparry calcite cement, stained pink, fill in the intercrystalline porosity. (e) A replacive, fine- to medium-grained subhedral dolomite occurs in patches of burrow-like fabric. (f) Structureless, fine- to medium-crystalline and subhedral to anhedral dedolomite (stained pink) replaced the precursor dolomite. (For interpretation of the references to color in this figure legend, the reader is referred to the web version of this article.)

4.4. Stratigraphic architecture and depositional model

The stratigraphic architecture of the Jubaila Formation has been reconstructed combining the bedding pattern and stratal geometries with a detailed facies observations of studied sections. The depositional evolution incorporated two stages of development comprises the transgressive and highstand deposits of a fourth-order depositional sequence Vail et al. (1991), related to eustatic sea-level changes. The first stage of the depositional evolution represents the deepest part of the formation and reveals an overall transgressive–regressive trend. The lower part of the Jubaila Formation consists of horizontally-bedded mid-outer ramp facies that are characterized by small-scale stacked cycles of mudstone interbedded fining-upwards wackestone–mudstone beds, composed of sponge spicules, radiolarians and brachiopod fragments with frequent mottled firm grounds and hard grounds. Overlying distal mid-ramp facies are characterized by wavy-bedding of mollusk-coated grain–intraclast sandy rudstone with thin storm beds and bioclastic tempestites. Bioclasts increase upward through the section but they are usually broken and mixed with significant amounts of siliciclastic clasts as a result of reworking by storms. The mid-outer ramp facies grade upwards into shallow subtidal proximal mid-ramp facies that are characterized by *Cladocoropsis*-intraclast–peloidal–bioclastic packstone/grainstone facies. The shallow subtidal proximal mid-ramp facies are interbedded with planar cross-bedded and cross-laminated, coarse-grained and well sorted limestones; including foram-bioclast–oncoid grainstone/rudstone and foram-bioclast-peloidal packstone/grainstone of ramp crest facies. Above the deep subtidal facies, the succession passes up sharply into shallow-water carbonate platform facies that reflect overall regressive trend (stage 2). The shallow-water carbonate deposits consist of erosionally based

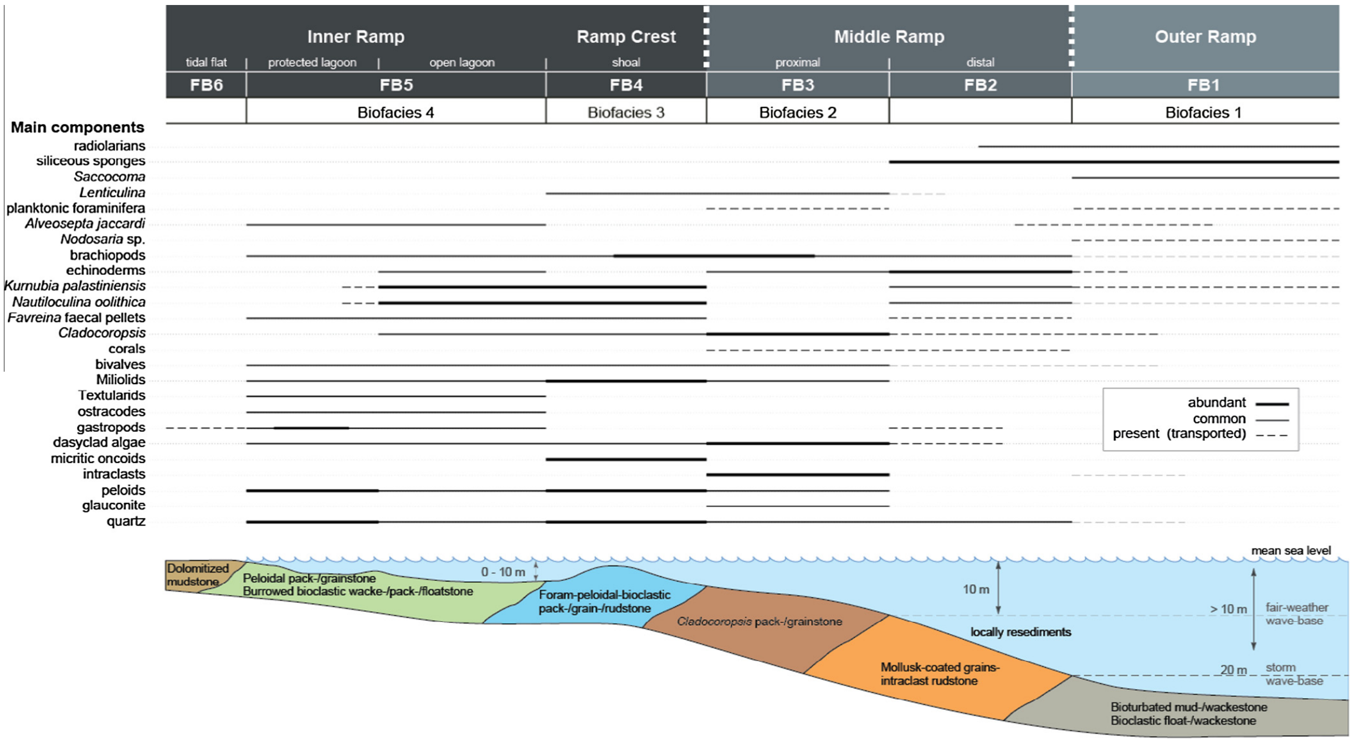

Fig. 11. Facies model for the Upper Jurassic Jubaila Formation showing the distribution of mud- and grain-supported facies and characteristic constituents.

shallow channels filled with reworked stromatoporoids and are interbedded with several packages of dolomites and dedolomites (Meyer et al., 1996). The bedding within this part of the succession shows a thickening upwards that suggests shallowing upwards. The uppermost part of the Jubaila Formation arranged into meter-scale coarsening-upwards cycles ranged from laminated dolomitic mudstone and wackestone to stromatoporoid packstone/floatstone/rudstone into bioclastic intraclastic peloidal packstone and grainstone. The laminated dolomitic mudstones that form the deepest parts of the shallowing-upward subtidal cycles would have been deposited in the distal mid-ramp setting. Farther upwards lagoonal facies re-appear and include peloidal packstone/grainstone facies, burrowed bioclastic wackestone/floatstone facies, and peloidal bioclastic packstone/floatstone. This passes upward into thin tidal-flat facies and chaotic breccias.

5. Conclusions

The succession of the Jubaila Formation has been ascribed to a carbonate ramp model in the Central Arabian Arch. This interpretation is supported by the features of the 4 biofacies and 12 microfacies that have been identified. The suggested depositional model relates the facies and biofacies to a down dip depositional profile of an inner, middle to outer carbonate ramp. The mudstone and wackestone facies (F1a–F1b) and the associated *Lenticulina*-spicule assemblage 1 reflect a distal middle to outer ramp (FB1). The mollusk-coated grains–intraclast sandy rudstone (F2) characterize the distal middle ramp. The *Cladocoropsis*-intraclast–peloidal–bioclastic limestone facies (F3a–F3b) and the commonly present *Cladocoropsis*–dasyclad algae assemblage imply deposition in sheltered proximal middle ramp. The planar cross-bedded and well sorted foram-bioclast–oncoid grainstone and rudstone (F4a–F4b) associated with foraminiferal-bioclast assemblage suggest accumulation in the highly energetic ramp-crest shoal environment. The burrowed bioclastic wackestone and floatstone and the associated foraminiferal assemblage, along with peloidal packstone/grainstone facies, laminated dolomitized peloidal packstone (F5a–F5d) indicate deposition in an inner ramp lagoon. The dolomitized mudstone and breccia (F6a–F6b) indicate a protected inner ramp in a tidal-flat environment.

The depositional evolution of the studied succession involved two stages reflecting a transgressive–regressive depositional sequence, which are strongly controlled by eustatic sea-level changes. The first stage is the deepest part of the formation and it represents an overall transgressive trend. Generally, the succession begins with small-scale stacked cycles of mudstones are dominated by sponge spicules, radiolarians and brachiopod fragments with frequent mottled firm ground and hard ground of a mid-outer ramp environment; these grade upwards to mollusk-coated grain–intraclast sandy rudstone facies characterized by thin storm beds and bioclastic lenses of distal mid-ramp deposits. Succeeding proximal mid-ramp consists of, *Cladocoropsis*-intraclast–peloidal–bioclastic packstone/grainstone is dominated by an open-marine fauna of branched stromatoporoids and calcareous algae mixed with intraclasts and peloids. Farther up, the succession becomes more shallow-marine with foram-bioclast–oncoid grainstone/rudstone and foram-bioclast-peloidal packstone/grainstone facies that represent ramp-crest shoal deposits. The second stage is represents the regressive part has a characteristic progradational trend. The shallow-water carbonate deposits arranged into meter-scale coarsening-upward cycles ranged from laminated dolomitic mudstone and wackestone to stromatoporoid packstone and rudstone into bioclastic intraclastic peloidal packstone and grainstone overlain by tidal-flat and chaotic breccias.

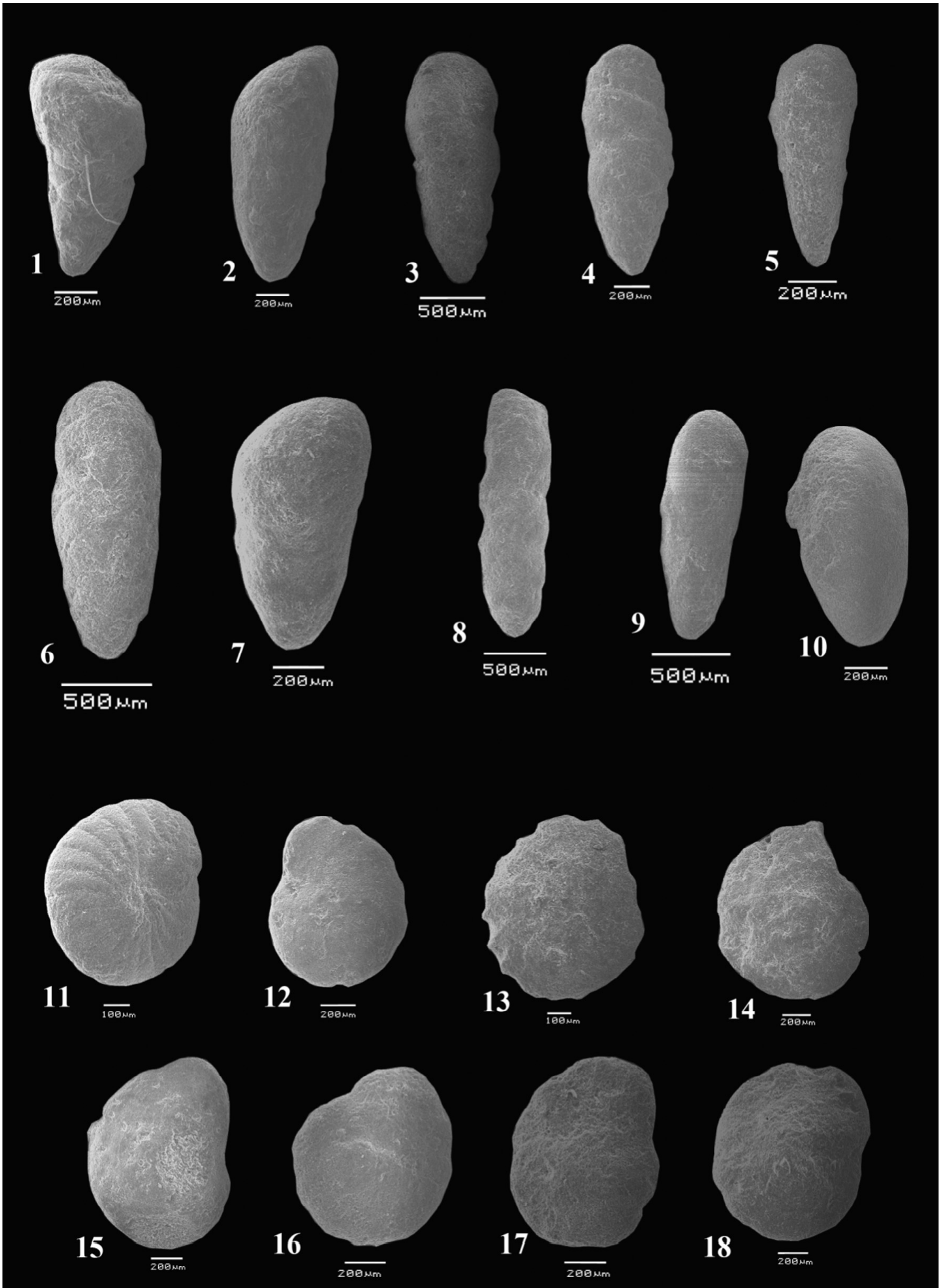

Fig. 12. (1, 2) *Palaeogaudryina magharaensis* (Said and Barakat); (3, 4, 8, 9) *Kurbubia palastiniensis* (Henson); (5) *Kurnubia wellingsi* (Henson); (6) *Praekurnubia jurassica* (Henson); (7) *Pfenderina neocomiensis* (Pfender); (10) *Haurania deserta* (Henson); (11) *Choffatella decipiens* (Schlumberger); (12) *Nautiloculina oolithica* Mohler; (13) *Evolutinella* sp.; (14) *Oolina globosa* (Montagu); (15, 16) *Lenticulina muensteri* (Roemer); (17, 18) *Nautiloculina circularis* (Said and Barakat).

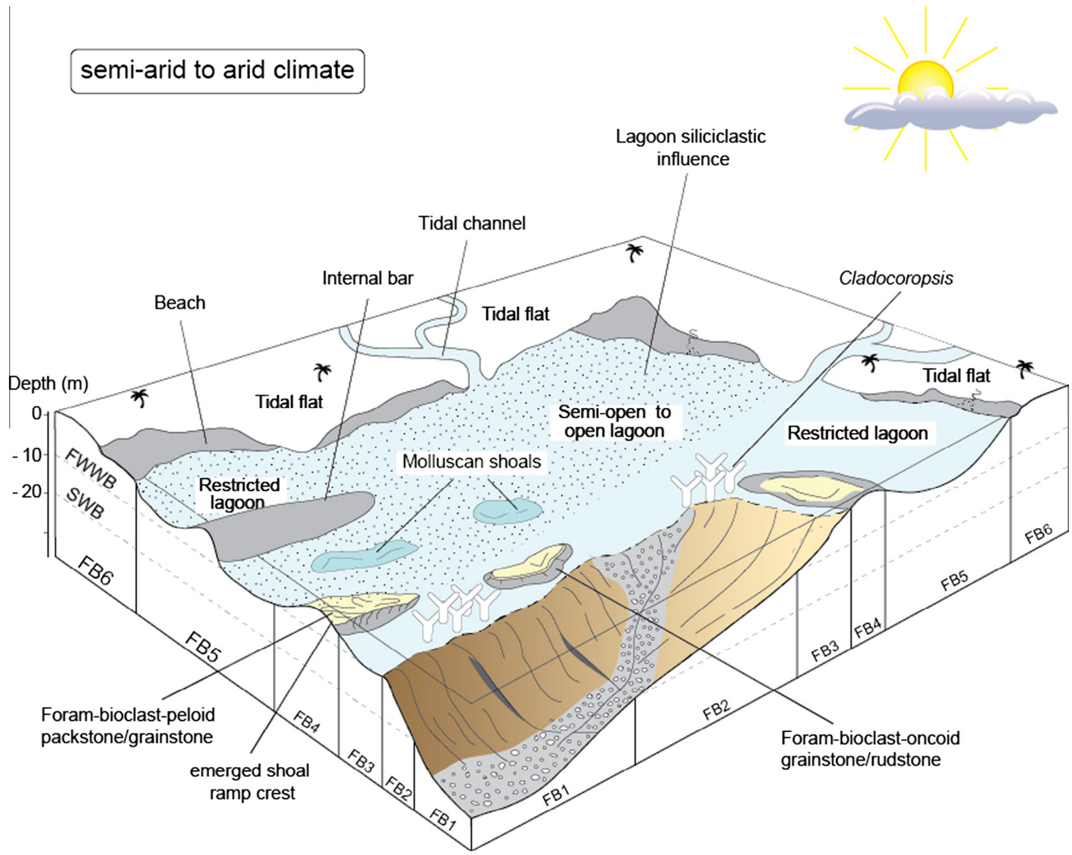

Fig. 13. 3D facies model (not to scale) of the studied carbonate ramp. This model illustrates the possible lateral distribution of different facies and facies belts. Note that not all facies associations necessarily coexist at a given time and configuration.

Acknowledgments

Authors would like to extend their sincere appreciation to the Deanship of Scientific Research at King Saud University for its funding this research group No. (RG-1435-033).

References

Adams, J.E., Rhodes, M.L., 1960. Dolomitization by seepage refluxion. Am. Assoc. Petrol. Geol. Bull. 44, 1912–1920.
AL-Saad, H., 2008. Stratigraphic distribution of the Middle Jurassic Foraminifera in the Middle East. Rev. Paléobiol. 27 (1), 1–13, Genève.
Al-Hashimi, W.S., Hemingway, J.E., 1973. Recent dedolomitization and the origin of the rusty crusts of Northumberland. J. Sediment. Petrol. 43, 82–91.
Al-Husseini, M.I., 1997. Jurassic sequence stratigraphy of the western and southern Arabian Gulf. GeoArabia 2, 361–382.
Al-Husseini, M.I., 2000. Origin of the Arabian plate structures: Amar collision and Najd Rift. GeoArabia 5, 527–542.
Alsharhan, A.S., Kendall, C.G., St, C., 1986. Precambrian to Jurassic rocks of the Arabian Gulf and adjacent areas; their facies, depositional setting and hydrocarbon habitat. Am. Assoc. Petrol. Geol. Bull. 70, 977–1002.
Alsharhan, A.S., Magara, K., 1995. Nature and distribution of porosity and permeability in Jurassic carbonate reservoirs of the Arabian Gulf Basin. Facies, Germany 32 (32), 37–254.
Ayres, M.G., Bilal, M., Jones, R.W., Slentz, L.W., Tartir, M., Wilson, A.O., 1982. Hydrocarbon habitat in main producing areas, Saudi Arabia. Am. Assoc. Petrol. Geol. Bull. 66, 1–9.
Burchette, T.P., Wright, V.P., 1992. Carbonate ramps depositional systems. Sediment. Geol. 79, 3–57.
Carrigan, W.J., Cole, G.A., Colling, E.L., Jones, P.J., 1995. Geochemistry of the Upper Jurassic Tuwaiq Mountain and Hanifa Formation petroleum source-rocks of eastern Saudi Arabia. In: Katz, B. (Ed.), Petroleum Source Rocks. Springer Verlag, pp. 67–87.
Droste, H., 1990. Depositional cycles and source-rock development in an epeiric intra-platform basin: the Hanifa Formation of the Arabian Peninsula. Sediment. Geol. 69, 281–296.
Dunham, R.J., 1962. Classification of carbonate rocks according to depositional texture. In: Ham, W.E. (Ed.), Classification of Carbonate Rocks, vol. 1. American Association of Petroleum Geologists Memoir, pp. 108–121.
El-Sorogy, A.S., Al-Kahtany, Kh., 2015. Contribution to the scleractinian corals of Hanifa Formation, Upper Jurassic, Jabal Al-Abakkayn Central Saudi Arabia. Hist. Biol. 27 (1), 90–102.
El-Sorogy, A.S., Al-Kahtany, Kh., El-Asmar, H., 2014. Marine benthic invertebrates of the Upper Jurassic Tuwaiq Mountain Limestone, Khashm Al-Qaddiyah, Central Saudi Arabia. J. Afr. Earth Sci. 97, 161–172.
Enay, R., Le Nindre, Y.-M., Mangold, C., Manivit, J., Vaslet, D., 1987. Le Jurassique d'Arabie Saoudite Centrale: Nouvelles donnes sur la lithostratigraphie, les paleoenvironnements, les faunes d'ammonites, les ages et les correlations. In: Enay, R. (Ed.), Le Jurassique d'Arabie Saoudite Centrale. Geobios Memoire Special 9, pp. 13–65.
Embry, A., Klovan, J.E., 1971. A Late Devonian reef tract on Northeastern Banks Island, N.W.T. Bull. Can. Petrol. Geol. 19, 730–781.
Flügel, E., 2004. Microfacies of Carbonate Rocks: Analysis, Interpretation and Application. Springer, 976 pp.
Galal, G., Kamel, S., 2004. Benthic Foraminifera from the Callovian Middle Jurassic Tuwaiq Formation, Central Saudi Arabia. J. Fac. Sci. 13, 57–72.
Handford, C.R., Cantrell, D.L., Keith, T.H., 2002. Regional facies relationships and sequence stratigraphy of a super-giant reservoir (Arab-D Member), Saudi Arabia. In: Armentrout, J.M. (Ed.), Sequence Stratigraphic Models for Exploration and Production: Evolving Methodology, Emerging Models and Application Histories. 22nd Annual Bob F. Perkins Research Conference: Gulf Coast Section SEPM, pp. 539–564.
Hughes, G.W., 2004. Middle to Upper Jurassic Saudi Arabian carbonate petroleum reservoirs: biostratigraphy, micropalaeontology and palaeoenvironments. GeoArabia 9, 79–114.
Hughes, G.W., 2006. Biofacies and palaeoenvironments of the Jurassic Shaqra Group of Saudi Arabia. Volumina Jurassica 4, 89–90.
Hughes, G., 2008. Biofacies and palaeoenvironments of the Jurassic Shaqra Group of Saudi Arabia. Volumina Jurassica 6, 33–45.
Hughes, G.W., Naji, N., 2008. Sedimentological and micropalaeontological evidence to elucidate post-evaporitic carbonate palaeoenvironments of the Saudi Arabian latest Jurassic. Volumina Jurassica 6, 61–73.
James, N.P., 1983. Reef environment. In: Scholle, P.A., Bebout, D.G., Moore, C.H. (Eds.), Carbonate Depositional Environments, vol. 33. American Association Petroleum Geologists Memoir, pp. 345–440.
Jones, B., 2007. Inside-out dolomite. J. Sediment. Res. 77, 539–551.

Jones, B., Desrochers, A., 1992. Shallow platform carbonates. In: Walker, R.G., James, N.G. (Eds.), Facies Models: Response to Sea Level Change. Geological Association of Canada, pp. 277–301.
Konert, G., Al-Afifi, A.M., Al-Hajri, S.A., 2001. Paleozoic stratigraphy and hydrocarbon habitat of the Arabian Plate. GeoArabia 6, 407–442.
Kuznetsova, K.I., Grigelis, A.A., Adjamian, J., Jarmakani, E., Hallaq, L., 1996. Zonal Stratigraphy and Foraminifera of the Tethyan Jurassic (Eastern Mediterranean). Gordon and Breach Publishers, 256 p.
Leinfelder, R.R., Schlagintweit, F., Werner, W., Ebli, O., Nose, M., Schmid, D.U., Hughes, G.W., 2005. Significance of stromatoporoids in Jurassic reefs and carbonate platforms—concepts and implications. Facies 51, 287–325.
Le Nindre, Y.-M., Manivit, J., Manivit, H., Vaslet, D., 1990. Sequential stratigraphy of the Central Saudi Arabian platform in the Jurassic and Cretaceous. Ministry of Petroleum and Mineral Resources, Directorate General of Mineral Resources, Jeddah, Saudi Arabia, Technical Report BRGM-TR-11-4, 11 p.
Lindsay, R.F., Cantrell, D.L., Hughes, G.W., Keith, T.H., Mueller, H.W., Russell, S.D., 2006. Ghawar Arab-D reservoir: widespread porosity in shoaling-upward carbonate cycles, Saudi Arabia. In: Harris, P.M., Weber, L.J. (Eds.), Giant Hydrocarbon Reservoirs of the World: From Rocks to Reservoir Characterization and Modeling. AAPG Memoir 88/SEPM Special Publication, pp. 97–137.
Melim, L.A., Scholle, P.A., 2002. Dolomitization of the Capitan Formation forereef facies (Permian, west Texas and New Mexico): seepage reflux revisited. Sedimentology 49, 1207–1227.
Manivit, J., Pellaton, C., Vaslet, D., Le Nindre, Y.-M., Brosse, J.-M., Fourniguet, J., 1985. Geologic map of the Wadi al Mulayh Quadrangle, Sheet 22H, Kingdom of Saudi Arabia. Saudi Arabian Deputy Ministry for Mineral Resources Geosciences Map, GM-92, Scale 1:250,000, pp. 1–32.
Manivit, J., Pellaton, C., Vaslet, D., Le Nindre, Y.-M., Brosse, J.-M., Breton, J.-P., Fourniguet, J., 1985. Geologic map of the Darma Quadrangle, Sheet 24H, Kingdom of Saudi Arabia. Saudi Arabian Deputy Ministry for Mineral Resources Geosciences Map, GM-101, Scale 1:250,000, pp. 133.
Manivit, J., Vaslet, D., Berthiaux, A., Le Strat, P., Fourniguet, J., 1986. Geologic map of the Buraydah Quadrangle, Sheet 26G, Kingdom of Saudi Arabia. Saudi Arabian Deputy Ministry for Mineral Resources Geosciences Map, GM-114, Scale 1:250,000, pp. 1–32.
Meyer, F.O., Price, R.C., Al-Ghamdi, I.A., Al-Goba, I.M., Al-Raimi, S.M., Cole, J.C., 1996. Sequential stratigraphy of outcropping strata equivalent to Arab-D reservoir, Wadi Nisah, Saudi Arabia. GeoArabia 1, 435–456.
Murris, R.J., 1980. Middle East: stratigraphic evolution and oil habitat. Am. Assoc. Petrol. Geol. Bull. 64, 597–618.
Nader, F.H., Swennen, R., Keppens, E., 2008. Calcitization/dedolomitization of Jurassic dolostones (Lebanon): results from petrographic and sequential geochemical analyses. Sedimentology 55, 1467–1485.
Powers, R.W., 1968. Lexique Stratigraphique International, v.III, Asie, 10bl, Saudi Arabia. Centre National de la Recherche Scientifique, Paris, 177p.
Powers, R.W., Ramirez, L.F., Redmond, C.D., Elberg, E.L., 1966. Geology of the Arabian Peninsula, Geological Survey Professional Paper, 560-D, 147p.
Purser, B.H., Brown, A., Aïssaoui, D.M., 1994. Nature, origin and evolution of porosity in dolomites. In: Purser, B.H., Tucker, M.E., Zenger, D.H. (Eds.), Dolomites – A Volume in Honour of Dolomieu, vol. 21. IAS Special Publication, pp. 283–308.
Qing, H., Bosence, D.W.J., Rose, E.P.F., 2001. Dolomitization by penesaline sea water in Early Jurassic peritidal platform carbonates, Gibraltar, western Mediterranean. Sedimentology 48, 153–163.
Read, J.F., 1982. Carbonate platforms of passive (extensional) continental margin: types, characteristics and evolution. Tectonophysics 81, 195–212.
Read, J.F., 1985. Carbonate platforms facies models. Am. Assoc. Petrol. Geol. Bull. 69, 1–21.
Read, J.F., 1989. Controls on evolution of Cambrian-Ordovician passive margin, US Appalachians. In: Crevello, P.D., Wilson, J.L., Sarg, J.F., Read, J.F. (Eds.), Controls on Carbonate Platform and Basin Development, vol. 44. SEPM Special Publication, pp. 146–165.
Sharland, P., Archer, R., Casey, D., Davies, R., Hall, S., Heward, A., Horbury, A., Simmons, M., 2001. Arabian Plate Sequence Stratigraphy: Mesozoic and Cenozoic sequences. GeoArabia Special Publication 2, 371p.
Steineke, M., Bramkamp, R.A., 1952. Stratigraphical introduction. In: Arkell, W.J., Bramkamp, R.A., Steineke, M. (Eds.), Jurassic Ammonites from Jebel Tuwaiq, Central Arabia. Royal Society [London] Philosophical Transactions B, vol. 236, pp. 241–313.
Steineke, M., Bramkamp, R.A., Sander, N.J., 1958. Stratigraphic Relations of Arabian Jurassic Oil. In: American Association of Petroleum Geologists Symposium, Tulsa, pp. 1294–1329.
Swart, P.K., Cantrell, D.L., Westphal, H., Handford, C.R., Kendall, C.G., St, C., 2005. Origin of dolomite in the Arab-D reservoir from the Ghawar Field, Saudi Arabia: evidence from petrographic and geochemical constraints. J. Sediment. Res. 75, 476–491.
Tucker, M.E., Wright, V.P., 1990. Carbonate Sedimentology. Blackwell, Oxford, p. 527.
Vail, P.R., Audemard, F., Bowman, S.A., Eisnet, P.N., Perez-Cruz, C., 1991. Signatures of tectonics, eustasy and sedimentology – an overview. In: Einsele, G., Ricken, W., Seilacher, A. (Eds.), Cycles and Events in Stratigraphy. Springer, Berlin, pp. 617–659.
Vaslet, D., Delfour, J., Manivit, J., Le Nindre, Y.M., Brosse, J.M., Fourniquet, J., 1983. Geologic map of the Wadi ar Rayn quadrangle, Sheet 23H, Kingdom of Saudi Arabia. Saudi Arabian Deputy Ministry for Mineral Resources, Jeddah, Geosciences Map, GM-63A.
Vaslet, D., Pellaton, C., Manivit, J., Le Nindre, Y.-M., Brosse, J.-M., Fourniquet, J., 1984. Explanatory Notes to the Geologic Map of the Sulayyimah Quadrangle, Sheet 24 H, Kingdom of Saudi Arabia. Saudi Arabian Deputy Ministry for Mineral Resources, Jeddah, Geosciences Map, GM-100A.
Vaslet, D., Al-Muallem, M.S., Maddeh, S.S., Brosse, J.-M., Fourniquet, J., Breton, J.-P., Le Nindre, Y.-M., 1991. Explanatory notes to the geologic map of the Ar Riyad Quadrangle, Sheet 24 I, Kingdom of Saudi Arabia. Saudi Arabian Deputy Ministry for Mineral Resources, Jeddah, Geosciences Map, GM-121.
Wright, V.P., Burchette, T.P., 1996. Shallow-water carbonates environment. In: Reading, H.G. (Ed.), Sedimentary Environments: Processes, Facies, Stratigraphy, pp. 325–394.
Youssef, M., El-Sorogy, A., 2015. Palaeoecology of benthic foraminifera in coral reefs recorded in the Jurassic Tuwaiq Mountain Formation of the Khashm Al-Qaddiyah Area, Central Saudi Arabia. J. Earth Sci. 26 (2), 224–235.
Ziegler, M.A., 2001. Late Permian to Holocene paleofacies evolution of the Arabian Plate and its hydrocarbon occurrences. GeoArabia 6, 445–504.